

Zhang *et al.*

Identification and Analysis of Over 2000 Ribosomal Protein Pseudogenes In the Human Genome

Zhaolei Zhang, Paul Harrison and Mark Gerstein*

Department of Molecular Biophysics and Biochemistry, Yale University, 266 Whitney Avenue,
New Haven, CT 06520-8114

*Corresponding author

Tel: (203) 432 6105

Fax: (360) 838 7861

Email: Mark.Gerstein@yale.edu

Keywords: pseudogene, ribosomal protein, genome, bioinformatics

ABSTRACT

Mammals have 79 ribosomal proteins (RP). Using a systematic procedure based on sequence homology search, we have comprehensively identified pseudogenes of these proteins in the human genome. Our assignments are available at <http://www.pseudogene.org/> or <http://bioinfo.mbb.yale.edu/genome/pseudogene>. In total, we found 2090 processed pseudogenes and 16 duplications of RP genes. The processed pseudogenes have average relative sequence length of 97% to the matching protein and average sequence identity of 76%. A small number (258) of them do not contain obvious disablements (stop codons or frameshifts) and thus could be mistaken as functional genes. On average, processed pseudogenes have longer truncation at the 5' end than the 3' end, consistent with a target primed reverse transcription (TPRT) mechanism. 178 of the processed pseudogenes are disrupted by one or more repetitive elements. Interestingly, on chromosome 16, an RPL26 processed pseudogene was found in the intron region of a functional RPS2 gene. The large-scale distribution of RP pseudogenes throughout the genome appears chiefly to result from random insertions with the numbers on each chromosome, consequently, proportional to its size. In contrast to RP genes, the RP pseudogenes have the highest density in GC-intermediate regions (41-46%) of the genome, with the density pattern being between that of LINES and Alus. This can be explained by a negative selection theory as we observed that GC-rich RP pseudogenes decay faster in GC-poor regions. Also, we observed a correlation between the number of processed pseudogenes and the GC content of the associated functional gene, i.e. relatively GC-poorer RPs have more processed pseudogenes. This ranges from 145 pseudogenes for RPL21 down to 3 pseudogenes for RPL14. We were able to date the RP pseudogenes based on their sequence divergence from present-day RP genes, finding an age distribution similar to that for Alus. The distribution is consistent with a decline in retrotransposition activity in the hominid lineage during the last 40 Myr. We discuss the implication for retrotransposon stability and genome dynamics based on these new findings.

INTRODUCTION

All the proteins in the cell are synthesized by the ribosomes, large complexes of RNA and protein molecules. A typical mammalian cell has about 4×10^6 ribosomes, each is composed of four RNA molecules (rRNA) and 79 ribosomal proteins (RP). In total, ribosomes constitute about 80% of the RNA and 5-10% of the protein in a cell (Kenmochi *et al.* 1998). Great progress has been made in recent years in elucidating the structure and mechanism of the ribosome. The peptide sequence of the complete set of mammalian RPs have been deduced by Wool and colleagues (Wool *et al.* 1995), and the genes encoding all human RPs have been positioned on the human genetic map (Kenmochi *et al.* 1998; Uechi *et al.* 2001; Yoshihama *et al.* 2002). Moreover, several high-resolution atomic structures are now available for archaeal ribosomes (Ban *et al.* 2000; Schlutzen *et al.* 2000; Wimberly *et al.* 2000; Yusupov *et al.* 2001).

Although it is well recognized that rRNA catalyzes the basic biochemistry of protein synthesis, ribosomal proteins are important in facilitating rRNA folding, protecting them from nucleases, and coordinating the multi-step process of protein synthesis. Some RPs have substantial extra-ribosomal functions as well (Wool 1996). It is believed that RPs from all three kingdoms of life are related, probably having evolved from the same ancestral set of proteins after the conversion of the ribosome from an RNA complex to a ribonucleoprotein particle (RNP). Among eukaryotes, the number and sequence of cytoplasmic RPs are fairly well conserved. For instance, yeast and rat share all but one RP, and the sequence identity of their RPs ranges from 40% to 88%, with an average of 60%. Among mammals, the amino acid sequences of the RPs are almost identical. For example, for the 72 RPs of which amino acid sequences are available for both human and rat, the average sequence identity is 99%, and 32 of them are perfectly identical (Wool *et al.* 1995).

Zhang *et al.*

In the yeast cell, the 78 ribosomal proteins are encoded by 137 genes since 59 of the genes are duplicated (Planta & Mager 1998). In all cases, both gene copies are transcribed although their expression levels often differ considerably (Raue & Planta 1991). The proteins encoded by duplicated genes have identical or virtually identical sequences and are functionally indistinguishable. In contrast, it is widely recognized that in mammals a single gene encodes each RP, although most if not all of the RP genes have a number of processed pseudogenes located elsewhere in the genome. The existence of these pseudogenes has greatly hindered the sequencing and mapping efforts of human RP genes, so special intron-trapping strategy had to be undertaken to differentiate the real transcribed RP gene and pseudogenes (Kenmochi *et al.* 1998; Uechi *et al.* 2001). A number of RP genes have also been implicated in various human diseases: such as RPS19 in Diamond-Blackfan anemia (DBA) (Draptchinskaia *et al.* 1999), RPL6 in Noonan syndrome (Kenmochi *et al.* 2000) and RPS4X gene in Turner's syndrome (Zinn *et al.* 1993).

In general, pseudogenes are disabled copies of functional genes that do not produce a functional, full-length protein (Mighell *et al.* 2000; Vanin 1985). The disablements can take the form of premature stop codon or frame shift in the protein-coding sequence (CDS), or less obviously, deleterious mutations in the regulatory regions that controls gene transcription or splicing. There are two main types of pseudogenes: duplicated (non-processed) and processed. Duplicated pseudogenes arise from genomic DNA duplication or unequal crossing-over. They have the same general structure as functional genes, with sequences corresponding to exons and introns in the usual locations. Processed pseudogenes result from retrotransposition, i.e. reverse-transcription of mRNA transcript followed by integration into genomic DNA, presumably in the germ line. Because of their origin, processed pseudogenes are sometimes considered as a special type of retrotransposons just like Alu and LINE elements, or sometimes referred to as retro-pseudogenes. They are typically characterized by complete lack of introns, the presence of small flanking direct repeats and a polyadenine tract near the 3' end (provided that they have not decayed). Processed

Zhang *et al.*

pseudogenes in general are not transcribed, however in very rare cases, transcripts of some pseudogene have been reported though the functional relevance of these pseudogene transcripts remains unclear (Fujii *et al.* 1999; McCarrey *et al.* 1996; Olsen & Schechter 1999).

It is unclear how many pseudogenes exist in the human genome. Estimates for the number of human genes range from ~22,000 to ~75,000 (Crollius *et al.* 2000; Ewing & Green 2000; Harrison *et al.* 2002b; Lander *et al.* 2001; Venter *et al.* 2001). From previous reports, it is thought that up to 22% of these gene predictions may be pseudogenic (Lander *et al.* 2001; Yeh *et al.* 2001). It is important to characterize the human pseudogene population as their existence interferes with gene identification and annotation. They are also an important resource for the study of the evolution of protein families, e.g., studies on the human olfactory receptor sub-genome (Glusman *et al.* 2001). Previously, Harrison *et al.* performed a detailed analysis of pseudogenes on human chromosomes 21 and 22 (Harrison *et al.* 2002a). It was discovered that the protein family that has the largest number of processed pseudogenes were ribosomal proteins, a total of 43 were found on the two smallest human chromosomes. This extrapolated to over 2000 RP pseudogenes in the whole human genome.

We have developed a pipeline of mostly automatic procedures that enables us to discover and characterize pseudogenes quickly and comprehensively. Here we report the identification of over 2400 processed RP pseudogenes and pseudogenic fragments on the latest human genome draft sequence (Lander *et al.* 2001). Complete sequence and precise chromosomal location have been obtained for each pseudogene. We provide a comprehensive characterization of the human RP pseudogene population and discuss its implications for retrotransposition and genome dynamics.

RESULTS

Human Genome Has 2090 RP Processed Pseudogenes

We have conducted a comprehensive search for cytosolic ribosomal protein (RP) pseudogenes on the August 2001 freeze of the human genome draft (Lander *et al.* 2001). Details of the annotation procedure are described in the Methods section and a flow chart is shown in Figure 8A. Table 1 shows the distribution of identified RP pseudogenes among 22 autosomes and 2 sex chromosomes, together with the length of each chromosome and the number of functional RP genes previously mapped onto it (Kenmochi *et al.* 1998; Uechi *et al.* 2001; Yoshihama *et al.* 2002). Some general statistics of the processed pseudogene population are shown in Table 2. A total of 2090 processed RP pseudogenes were identified in the whole human genome. The substantial majority (1912) of these are termed “intact” pseudogenes since they are continuous in sequence with insertions shorter than 60 bp, while the remaining 178 are disrupted by long insertions in the middle of their sequence. The majority (146 of 178) of these disruptions are caused by the insertions of one or more retrotransposons, Alu, or less often, LINE elements.

358 pseudogenic fragments

We also found 358 pseudogenic fragments, which are continuous in sequence but produce transcripts shorter than 70% of a full-length RP peptide. On average these fragments match to 40% of the full-length RPs with an average amino acid sequence identity of 74.2% (see Table 2). There are three possible explanations for these short fragments. (i) They could have originally been individual exons of duplicated RP genes. (ii) They could have been intact processed pseudogenes and later became truncated by spontaneous DNA deletion or retrotransposon insertion. (iii) They could have been caused by premature termination of the reverse transcription process, which would lead to incomplete incorporation of cDNA into the chromosome. Because

Zhang *et al.*

the reverse-transcription starts at the 3' end (poly-A tail), such premature truncation would tend to occur at the 5' end of the cDNA sequence. The first scenario involves duplicated RP genes, and the last two scenarios assume a processed origin for the pseudogenic fragments. We believe the last two are more likely since there are evidences for both hypotheses. For most of these pseudogenic fragments, we could locate a retrotransposon within 300 bps on the chromosome with the average distance between the fragments and the retrotransposon being 108 bp. This close proximity strongly indicates retrotransposon insertion events in past evolution, which caused the RP pseudogene truncation. Also, the average truncation at 5' end for these fragments is almost two-fold longer than at 3' end (227 vs. 127 bp), which is consistent with the mechanism of target primed reverse transcription (Table 2). Based on these arguments, we counted these pseudogenic fragments as processed when we computed pseudogene density (see Table 1 caption), but in general these fragments were treated separately from the full-length processed pseudogene population. As the total number of these fragments is much smaller than the number of processed pseudogenes (358 vs. 2090), exclusion of them from the processed pseudogene counts does not affect the conclusions one way or another.

Kenmochi and colleagues have previously sequenced most of the 80 human RP genes and mapped them onto individual cytogenic bands (Kenmochi *et al.* 1998; Uechi *et al.* 2001; Yoshihama *et al.* 2002). In our process of searching for processed pseudogenes, 72 of these 80 RP genes were located and their cytogenic locations were confirmed. In addition, 16 duplicated copies of these RP genes were also identified, mostly in the neighboring region of the original RP genes.

Overall Statistics of The Processed Pseudogenes

Since the ribosomal proteins are of various lengths, we measure sequence completeness by defining relative length as the ratio between the length of translated pseudogene and the length of

Zhang *et al.*

the corresponding functional ribosomal proteins. In general, the RP pseudogenes are well preserved, as they tend to be almost full-length in their coding regions (96.5%), with high sequence identity in terms of both translated amino acid sequence (76.2%) and also underlying nucleotides (86.8%). Figure 1A illustrates the distribution of the relative sequence length of processed pseudogenes. Surprisingly, although we used 70% as a threshold to separate the processed pseudogenes from pseudogenic fragments, the CDS of majority of the processed pseudogenes (>90% of the set) are practically full-length. It is known that LINE1 reverse-transcriptase (RT) has a low efficiency that often leads to 5' truncation and thus incomplete insertion of transcripts. It is a little surprising that we have observed such a high percentage of near-complete pseudogenes, but it is probably because RT truncations mostly occurred in the 5' UTR instead of the protein-coding region. Figure 1B shows the distribution of DNA sequence identity between processed pseudogenes and the RP cDNA sequences. Figure 1C shows the distribution of number of disablements (premature stop codons and frame shifts) per pseudogene, with the y-axis plotted in log scale. Of the 1912 "intact" processed pseudogenes (Table 1), 258 (13%) do not contain any disablements; therefore they could potentially be mistaken as functional genes by some automatic gene prediction algorithms. The graph shows an exponential relationship. A similar exponential relationship has been previously observed in a smaller set of human olfactory pseudogenes (~ 600) (Glusman *et al.* 2001), and was interpreted in such a way to support an alternative origin for olfactory receptor pseudogenes other than gene duplication or retrotransposition.

We also checked the existence of polyadenine tail for our processed pseudogene set. Out of the 2090 processed pseudogenes, 952 (45.5%) have no obvious polyadenine tail of at least 30 bp detected (see Methods section), 176 (8%) have both a poly-A tail and a polyadenylation signal (mostly AATAAA) within 50 bp of the poly-A tail. 32 pseudogenes (1.5%) have the poly-A tail and the polyadenylation signal 50-100 bp upstream. 903 pseudogenes (44.5%) only have poly-A

Zhang *et al.*

tail with no detectable polyadenylation signal. We are confident in our assignment of processed pseudogenes; lack of poly-A tail for about half of the assigned processed pseudogenes can be explained as decay in genome sequence and nucleotide substitutions. Previously, Harrison *et al.* (Harrison *et al.* 2002a) found polyadenylation for only 52% of the processed pseudogenes on chromosomes 21 and 22, which is similar to the ratio we found here for RP pseudogenes.

Distribution of Pseudogenes Among Chromosomes

Unlike in prokaryotes, where the RP genes are organized into operons, the distribution of RP genes among human chromosomes is dispersed but not random (Feo *et al.* 1992; Kenmochi *et al.* 1998; Uechi *et al.* 2001; Yoshihama *et al.* 2002). Every human chromosome, except chromosome 7 and 21, contains at least one or more RP genes. Chromosome 19, one of the smallest chromosomes, contains as many as 13 RP genes (Table 1). Such high density of RP genes on chromosome 19 can be explained by the high chromosome GC content, which results in unusual high gene density (Lander *et al.* 2001; Mouchiroud *et al.* 1991; Venter *et al.* 2001). The distribution of processed RP pseudogenes in human genome appears more random and uniform than their functional counterparts (Figure 2). It is obvious that the abundance of processed pseudogenes on each chromosome is proportional to the chromosome length (Figure 3A), with a correlation coefficient of 0.89 ($P < 1E-8$). Including pseudogenic fragments in the set has no noticeable effect on this result.

We further calculated the RP pseudogene density (number of pseudogenes per Mb) for each chromosome and plotted them against chromosomal GC content (Figure 3B), which shows a weak positive correlation (correlation coefficient = 0.51, $P < 0.01$). The outlier on the bottom of the graph is the sex chromosome Y, which has the lowest pseudogene density even for its relatively low GC content. Chromosome Y is unusual in many ways as it also has the lowest density for Alu repeats (Lander *et al.* 2001). Lander *et al.* suggested that these phenomena might

Zhang *et al.*

be related to the high tolerance for DNA insertion and deletion and rapid gene turnover rate on this chromosome. If we weight the chromosome length by its GC content, then the correlation with the pseudogene density increased from 0.89 to 0.91 ($P < 1E-9$). It is likely that the chromosomal GC-content reflects the relative stability of the chromosome, i.e. pseudogenes are more likely to be preserved on the chromosomes that have a slower gene turnover rate.

Genomic Distribution of Processed Pseudogenes

Using a 100 Kb long, non-overlapping window, we divided human genome into over 30,000 segments and assigned them to five classes according to their average GC content. For each class, we also calculated the gene or pseudogene density by dividing the number of genes or pseudogenes by the amount of DNA in that class (Table 3). It is well established that in human genome, gene density is strongly correlated with local GC content, with the GC rich regions being mostly gene-dense (Lander *et al.* 2001; Mouchiroud *et al.* 1991; Venter *et al.* 2001). It is clearly the case for functional RP genes, as the GC-rich classes (> 46%) contain the majority of the RP genes and have higher RP gene density. In contrast, the RP pseudogenes are enriched in classes with lower GC content; they have the highest density in the genomic region with intermediate GC content (41-46%). In fact, the class that has the highest local GC-content (>52%) contains the fewest number of pseudogenes, although it has the highest RP gene density. Similar genomic distributions have previously been reported for chromosome 22 with a smaller set of 114 pseudogenes (Pavlicek *et al.* 2001). Our results suggest this is probably a general rule for all processed pseudogenes in the human genome.

It has been proposed that the protein machinery encoded by LINE1 element is involved in the arising of both the Alu repeats, LINE repeats (Feng *et al.* 1996; Jurka 1997; Weiner 1999) and the processed pseudogenes (Esnault *et al.* 2000; Weiner 1999). LINEs and Alus are the most frequent retrotransposons found in the human genome, each occupying about 15% and 10% of the genome

Zhang *et al.*

respectively. LINEs (Long Interspersed Elements) are about 6kb long and encode two open reading frames (ORFs). Alus are a major class of SINEs (Short Interspersed Elements), approximately 280 bp in length. Despite their common origin, the Alus in the human genome are predominantly found in GC-rich regions while LINEs and processed pseudogenes are more prevalent in relatively GC-poor regions. In this sense, the distribution of Alus is more similar to that of genes than pseudogenes. In Figure 4A, we plotted the RP pseudogene density along with the densities of functional RP genes, Alus and LINEs. (The data for Alus and LINEs are from the results of Pavlicek *et al* (Pavlicek *et al.* 2001)). It is obvious that both the functional RP genes and the Alus are enriched in the GC-rich regions and depleted in the GC-poor regions. LINEs are predominantly found in genomic regions with the lowest local GC-content. The distribution of RP pseudogenes falls between these extremes, as they have the highest density in the regions with intermediate GC content (41-46%).

Negative Selection Theory

The puzzling contrast between the genomic distribution of Alus and LINEs has recently been explained by comparing the distribution of repeats of different age groups (Lander *et al.* 2001; Pavlicek *et al.* 2001). It has been observed that young Alus, similar to LINEs, were more frequently found in the GC-poor region than the more ancient Alu elements. Based on such findings, Pavlicek *et al* (Pavlicek *et al.* 2001) proposed a negative selection theory, which hypothesized that the enrichment of Alus in the GC rich region was the result of their higher stability in the compositionally matching environment. It is believed that when the retrotransposons were first integrated into the nuclear genome, both Alus and LINEs preferred GC-poor (AT-rich) region since the LINE1 reverse-transcriptase/endonuclease specifically targets TT|AAA insertion site. Because of the conspicuously higher GC content of Alus (~ 57 %), their existence in GC poor region would destabilize the chromosome. Therefore these Alus would be selected against to be either lost or, perhaps more likely, their nucleotide composition would have

Zhang *et al.*

drifted towards lower GC level and decayed into background genomic DNA and became unrecognizable.

We believe the aforementioned negative selection theory can also explain the pseudogene density distribution illustrated in Figure 4A. The GC content of RP CDS ranges from 42% to 63% with median at 51%, which is not as high as Alus, but still much higher than the LINE repeats (~ 42%) and genome-wide average (~41%). The average GC content for the RP pseudogene sequences is 47%, which is intermediate between the functional RP genes and genomic DNA. Therefore, at least for RP pseudogenes we have observed the drift in their GC content, which supports the negative selection hypothesis. We further divided RP processed pseudogenes into four groups according to the average GC-content in the 100 Kb genomic region surrounding each pseudogene. For each group, we calculated the average GC content for both the pseudogene sequences and also the coding sequence (CDS) of the functional RP genes they originated from. The results are plotted in Figure 4B, which clearly shows a greater drift for pseudogenes in GC-poor region than in GC-rich region, therefore the pseudogenes in GC-poor region appear more decayed than those in the GC-rich region. Such drift in nucleotide composition has been previously reported for silent mutation sites in mammalian MHC gene sequences (Eyre-Walker 1999) and interspersed repeats in human genome (Lander *et al.* 2001). In both studies, significantly more single nucleotide substitutions from G/C to A/T than from A/T to G/C have been observed. Despite the drift in composition, the majority of the processed RP pseudogenes still have GC content higher than their surrounding genomic sequences.

Age Distribution of Processed Pseudogenes

When mRNA transcripts were reverse-transcribed to become pseudogenes, they were immediately released from selection pressure. Therefore the amount of mutations they accumulated during evolution could be used to infer their ages. Because mammalian RP

Zhang *et al.*

sequences have stayed almost unchanged since rodents and primates diverged over 100 Myr ago (99% sequence identity between rats and human), we can safely use the present-day human RP sequence as the ancient RP gene sequences to calculate the divergence rate for the processed pseudogenes. The percentage of sequence divergence was converted into approximate age in millions of years (Myr) by using a constant substitution rate of 1.5×10^{-9} per site per year (Li 1997). It is known that substitution rate varies during evolution (Goodman *et al.* 1998; Lander *et al.* 2001), however we believe such simplified treatment is sufficient for our purpose.

The age distribution of human repetitive sequences has been previously analyzed (Lander *et al.* 2001; Smit 1999). Figure 5 shows the distribution of sequence divergences for RP pseudogenes together with LINE1 and Alu repeats; each increment in divergence represents roughly 6.7 Myr. The repeats data are from Arian Smit (personal communication). It is obvious that processed pseudogenes have an age distribution much more similar to Alu elements than to LINE1 elements although they were all processed by the same LINE1 machinery. Note LINE1s are mammalian-specific and Alus are primate-specific. The distribution for RP pseudogenes peaks at an evolutionary age corresponding to 8-10% sequence divergence, while Alus peak at 7% and LINE1 elements peak at both 4% and 21%. Interestingly, RP pseudogenes also have a shoulder at 17-18%, which could have been the consequence of the surge of LINE1 retrotransposition activity just a few million years before that. The rate of new processed pseudogenes generated in the human genome has slowed down since ~ 40 Myr ago, which was roughly the time before when human species diverged from gibbons. This coincides with the decline of new LINE1 elements and Alus in the genome. It has been proposed that the structure and dynamics of hominid populations are responsible for such decline in retrotransposon activity (Lander *et al.* 2001).

GC-Poor RP Genes Have More Processed Pseudogenes

Table 4 lists the number of processed pseudogenes among 79 ribosomal proteins, sorted in the descending order. The first two columns list the SWISSPROT ID (Bairoch & Apweiler 2000) for the human RPs, and the standard mammalian RP gene nomenclature (Mager *et al.* 1997). Also listed are the lengths of RP mRNA transcripts, coding sequence (CDS) and the CDS GC content, all retrieved from GenBank. On average, 26 processed pseudogenes are found for each RP gene; however, different RP genes have clearly very different propensity of generating processed pseudogenes. The distribution of numbers of processed pseudogenes among RP genes is strikingly skewed, although presumably for each RP only one functional gene exists (Wool *et al.* 1995). RPL21 has the most copies of processed pseudogenes at 145, which are about 50% more than that of RPL23A, which has the second-most at 85. Meanwhile 24 RP genes have less than 10 copies of processed pseudogenes each, MRPL14 has the fewest at 3. For those RP genes that have the most number of processed pseudogenes, we also checked their chromosomal locations to make sure they were not created from genomic duplication, i.e. these processed pseudogenes arose mostly independently.

We were curious whether the different processed pseudogene abundance among RP genes is correlated with the recent decline in retrotransposition activity. For the processed pseudogenes originated from the same RP gene, we further divided them into three groups according to their ages: < 40 Myr, 40-80 Myr, and > 80 Myr (Figure 6A). It is obvious that the age distribution of processed pseudogenes is similar for all 79 RP genes, i.e. there were no preferences for certain group of RP genes in different evolution period. The correlation between the number of young pseudogenes (< 40 Myr) and number of mid-age pseudogenes (40-80 Myr) per RP gene is 0.73 ($P < 1E-13$); the correlation between mid-age pseudogenes and old pseudogenes (> 80 Myr) is 0.68 ($P < 1E-11$).

Zhang *et al.*

It is also plausible that the differences in pseudogene abundance merely reflect the different ages for individual RP gene, as presumably genes that have been around longer will have more chance being reverse-transcribed to generate pseudogenes. To check this, we grouped RP genes into three groups according to their phylogenetic profile, i.e. some RP genes are unique to eukaryotes while others have homologues in eubacterial and archaeobacterial kingdoms (Wool *et al.* 1995). There appears to be no correlation between processed pseudogene abundance and the degree of ubiquity. Within eukaryotes, we also looked at the sequence identity between yeast RPs and human RPs, no correlation found there as well. The pseudogene abundance also has no correlation with the extra-ribosomal function of some of the RP genes (Wool 1996).

Previously Goncalves *et al.* (Goncalves *et al.* 2000) analyzed 249 processed pseudogenes, which correspond to 181 functional genes, and concluded that human genes that gave rise to processed pseudogenes in general share four features. They were (i) widely expressed, especially in germ line, (ii) highly conserved, (iii) short, and (iv) GC-poor. The first two criteria are trivial for ribosomal proteins as RPs are ubiquitous in all cell types and they are also the most highly conserved among eukaryotes and mammals (Wool *et al.* 1995). In general, RP genes have short mRNAs and short CDS as seen from Table 4, although there is no significant correlation between the number of processed pseudogenes and the mRNA length (correlation -0.01, $P < 0.93$) (Figure 6B) or the CDS length (correlation 0.04, $P < 0.73$). We would like to emphasize the lack of obvious correlation between gene length and pseudogene abundance, as it demonstrates that our pseudogene searching procedure did not systematically miss out short pseudogenes, i.e. the skewed pseudogene distribution is not an artifact. However, there is a significant inverse correlation between number of processed pseudogenes and the GC-content of RP gene CDS (correlation -0.41, $P < 0.0002$) as shown in Figure 6C, i.e. relatively GC-poorer RP genes tend to have more processed pseudogenes than GC-richer ones. It is not immediately obvious what is the mechanism behind the enrichment for the relatively GC-poor RP genes, since the arising of a

Zhang *et al.*

processed pseudogene involves multiple steps and the selection for GC-poor RP genes could have occurred at any step along the way. More on this topic will be discussed in the Discussion section.

Non-processed Pseudogenes and Duplicated RP Genes

We only found 16 duplicated RP genes in the human genome (Table 5), which share identical exon structure with previously characterized RP genes (Kenmochi *et al.* 1998; Uechi *et al.* 2001). This is in sharp contrast to the yeast genome, where most RP genes are duplicated and the duplicated genes are also transcribed and functional. Only one duplicated gene in the human genome (RPL13A) has an obvious disablement in the coding region; it is possible other duplicated RP genes may have hard-to-detect disablements in the UTR regions or introns. It is not clear whether these duplicated RP genes are transcribed in the cell although it is generally assumed only one gene is functional for each ribosomal protein (Kenmochi *et al.* 1998; Wool *et al.* 1995). The majority of the duplicated genes are in the vicinity of the original genes, therefore could not have been resolved from the original genes in the hybridization experiments. There are notable exceptions: RPL26, RPS27 and RPL3 have duplicated copies on separate chromosomes, while RPS4Y has a duplicated copy on the opposite end of the chromosome Y. Interestingly, the duplicated copies for RPL26, RPS27 and RPL3 genes have much longer introns than the mapped genes, which were caused by insertion of Alu or LINE repeats (with the exception of RPS27). It is likely the sequence difference in intron region is the reason that they were missed out in the hybridization experiments even though they are far apart from the mapped RP genes. Detailed analysis of these duplicated genes will be described in subsequent reports.

Our homology matching procedure located at least one intron-containing functional gene for all but 8 RP genes: RPP2, RPL4, RPL30, RPL35A, RPL38, RPL41, RPS7 and RPS27A. We did, however, find processed pseudogenes for these RP genes in the genome. These genes either

Zhang *et al.*

consist of short exons or their protein sequences are predominantly low-complexity, making them difficult to find by homology matching.

It is surprising to discover a processed RPL26 pseudogene in the intron region of the functional RPS2 gene on chromosome 16 (band p13.3, Contig AC005363.1.1.75108, Ensembl ID ENSG00000140988). RPS2 gene has 7 exons; the pseudogene resides in the third intron (1015 bp long), between residues 89 and 90 in the RPS2 protein sequence. Interestingly, there is also an Alu element at the 3' end of the pseudogene, about 100 bp away. The pseudogene itself is 357 bp long, corresponding to residues 14 to 141 of RPL26, having amino acid sequence identity of 49% and nucleotide sequence identity of 73% (Figure 7). It appears to be very ancient, has already lost its poly-A tail, and has sequence divergence of 0.28, which corresponds to more than 100 Myr old. Figure 7 shows the alignment of RPL26 sequences from several eukaryotic organisms together with this pseudogene. At 11 positions, the pseudogene has the same residue with the mammalian sequences but not with the invertebrates. Notice rat and human sequences are almost identical except at residue 100 where rat has an Arginine and human has a Histidine. Interestingly this RPL26 pseudogene also has a Histidine at that position; this suggests the pseudogene became part of the intron before the divergence of rodent and hominid species. It has been known that some RP genes contain Alu or LINE elements in the 3' or 5' UTR; to our knowledge this is the first case where a processed pseudogene is found in the intron region of another functional gene. This has implications for the origin and evolution of introns.

Online Database

The data and results discussed in this report can be accessed online at <http://www.pseudogene.org/> or <http://bioinfo.mbb.yale.edu/genome/pseudogene/>.

DISCUSSION

Significance of RP Pseudogenes

Characterizing ribosomal protein pseudogenes is valuable in many ways. (i) It will be tremendously useful in the study of functional RP genes. RP genes are implicated in many human genetic diseases such as Diamond-Blackfan anemia (Draptchinskaia *et al.* 1999), Noonan syndrome (Kenmochi *et al.* 2000) and Turner's syndrome (Zinn *et al.* 1993). The precise nucleotide sequence and chromosomal location of RP pseudogenes will certainly help researchers in designing probes specific to functional genes. (ii) Pseudogenes can also serve as genomic milestones, as they provide snapshots of RP sequences existing millions of years back in evolution. Such information will be valuable in studying ribosome biogenesis and the phylogenetic relationships between organisms. The discovery of an RPL26 pseudogene in the intron region of a functional RPS2 gene could certainly shed light on the evolution of both RP genes. (iii) From the perspective of studying retrotransposition, processed pseudogenes are just a special type of repetitive elements like Alus. However, processed pseudogenes are much more diverse in terms of sequence length, GC-content, and other features than traditional retrotransposons, which makes them useful in studying evolution and dynamics of genomes. To our knowledge, our RP pseudogenes are the largest set ever studied.

Comparing With Ensembl Annotations

The Ensembl database (<http://www.ensembl.org/>) is an automated system for genome-wide gene prediction and annotation, which has direct links to primary HGP data sources (Birney *et al.* 2001; Hubbard *et al.* 2002). The annotation process relies on matching genomic DNA sequence and GenScan peptides (Burge & Karlin 1997) with known proteins, mRNAs and other sequence information. All the genes have been checked to be transcribed before they were included into

Zhang *et al.*

the database (Daniel Barker, personal communications). As of end of February 2002, there were approximately 47,000 annotated genes in Ensembl, of which 549 were annotated as ribosomal protein genes. Some of these have more detailed annotations associating them with a particular RP such as “60S RIBOSOMAL PROTEIN L7”, others were described more loosely such as “60S RIBOSOMAL PROTEIN”. After re-aligning these genes with human RP protein sequences and removing some dubious matches, we derived a set of 481 Ensembl RP entries.

Ensembl doesn't explicitly differentiate between functional genes and pseudogenes, nor does it aim to (Daniel Barker, personal communication). Consequently, most of these 481 Ensembl RP entries turned out to be pseudogenes instead of functional genes, as only 260 (54%) translate to peptides longer than 95% of full-length ribosomal proteins. For instance, a gene ENSG00000150624 on chromosome 2 was annotated as “60S RIBOSOMAL PROTEIN L17”, but produced a transcript that was only 51.6% of the full-length RPL17, and had sequence identity of 56.2%. Moreover only 170 of these genes have introns; most of these Ensembl RP genes (64.6%) are single exons. We checked the overlap between our RP pseudogene sets with these Ensembl RP entries. 474 out of 481 (98.5%) Ensembl RP entries have significant overlaps with our pseudogenes and in most cases our pseudogenes were longer than the Ensembl entries. Five RPL41 single-exon processed pseudogenes from Ensembl were the only ones missed out by our procedure. The RPL41 is the shortest ribosomal protein, with only 25 amino acids; it also contains 17 near-consecutive Arginine and Lysine residues. It is likely that short length and low complexity caused BLAST to fail to detect these pseudogenes. Note that Ensembl is a database in flux, i.e. the sequence and annotation are continuously updated and improved. Therefore some of the examples and statistics given above will probably be out-of-date when this report is published. Nonetheless, the overlap in annotation of genes and pseudogenes documented above is important as it demonstrates the need to systematically include pseudogene identification in genome annotation efforts.

Automatic gene prediction programs alone do not have the ability of differentiating between functional genes and pseudogenes, especially if the pseudogenes do not contain obvious disablements in the coding sequence (CDS). Furthermore, for those pseudogenes that contain disablements, gene prediction programs either discard them or stop at the disablement and predict the pseudogene as a functional gene but with truncated length. We think this is the reason that so many RP pseudogenes were passed into Ensembl database as functional genes. It has been long debated on how many genes the human genome contains, as different methods such as EST analysis and GenScan (Burge & Karlin 1997) gave different estimates (Harrison *et al.* 2002b). It is probably not appropriate to extrapolate the over-estimation for RP genes onto the whole human proteome, as ribosomal proteins are a very unique protein family in many ways. Nevertheless, special care should be taken in interpreting outputs from automatic gene prediction programs.

Pseudogene Abundance Per RP Can Not Be Explained By Positive Selection

As mentioned previously, we found an inverse correlation between RP gene GC content and the pseudogene abundance for that gene (Figure 6C), i.e. the relatively GC-poor RP genes tend to have more processed pseudogenes. Before we go on discussing the possible mechanism behind this correlation, it helps to give a brief overview on the LINE1-mediated retrotransposition process, which is believed to be responsible for generating processed pseudogenes (Kazazian & Moran 1998). LINE1-mediated retrotransposition can be divided into four steps. (i) In the first step, a retrotransposon or gene is transcribed in the nucleus to produce an mRNA transcript. (ii) In the second step, the mRNA transcripts are transported into cytoplasm and LINE1 mRNA transcripts are translated into two proteins: ORF1 (also known as p40), and ORF2, which is a reverse-transcriptase/endonuclease. (iii) Human ORF1 has been demonstrated to be a sequence-specific single-strand RNA binding protein, which binds specifically but not exclusively to

Zhang *et al.*

LINE1 transcript to form a ribonucleoprotein particle (RNP) which also includes ORF2 protein (Hohjoh & Singer 1996; Hohjoh & Singer 1997b; Kazazian & Moran 1998; Leibold *et al.* 1990; Martin 1991; Moran *et al.* 1996). (iv) In the fourth step, the RNP particle migrates into nucleus and undergoes target-primed reverse-transcription, which give rise to a new retrotransposon or processed pseudogene.

If the GC-poor RP genes were selected favorably in retrotransposition (i.e. there is a positive selection for them), it must have occurred in one of the four steps described above. However, we cannot find any evidence for such positive selection in any of the steps. In relation to step (i), we have compared the processed pseudogene abundance per gene with the mRNA expression level in human and yeast cells (see Methods). No significant correlation between the datasets was found, suggesting the selection could not have occurred at the step of gene transcription. In relation to step (ii), lack of correlation between mRNA length and pseudogene abundance also suggested the transportation of RP transcript in and out of nucleus had no effect on retrotransposition. This is based on the idea that longer mRNAs are harder to transport. In relation to step (iii), the forming of RNP particle, it has been demonstrated that the binding between ORF1 and mRNA transcript has a *cis*-preference, i.e. ORF1 has higher affinity to wild-type LINE1 transcripts that encode it. However at a much lower level, ORF1 or ORF1 and ORF2 together can also act *in trans* to retrotranspose mutant LINEs and other mRNA transcripts, (Esnault *et al.* 2000; Hohjoh & Singer 1997a; Hohjoh & Singer 1997b; Wei *et al.* 2001). It is not clear what sequence or structural features on the mRNA transcripts constitute the *cis* and *trans* preference, though it is unlikely that the overall GC content is the deciding factor since Alu elements and LINE elements, two most populous retrotransposons in human genome, have very different GC content (56.8% for Alus and 42.3% for LINEs). Following the same reasoning, it is also unlikely the reverse-transcription in the fourth step has preference for GC-poor transcripts.

Zhang *et al.*

Negative Selection For GC-poor RP Genes In Retrotransposition

From above analysis we have found no evidence for a positive selection mechanism in retrotransposition of GC-poor RP genes; however, a negative selection mechanism can readily explain the skewed distribution. In this mechanism, the accumulation of GC-poor RP pseudogenes can be interpreted as the indirect result of faster decay rate for GC-rich RP pseudogenes in the GC-poor genome region where they were originally inserted.

Analogous to the mechanism of enrichment of Alu elements in the GC-rich region, which we described earlier in this report, the existence of GC-rich RP pseudogenes in the GC-poor genomic region was more unfavorable than GC-poor RP pseudogenes. Thus there would be greater selection pressure against these GC-rich pseudogenes. Pavlicek *et al.* (Pavlicek *et al.* 2001) divided Alu and LINE elements into different age groups and studied their distribution in genome regions of different GC-content. They showed the young Alus (divergence < 2% from consensus sequence) are indeed less depleted in the GC-poor region. This effect is not evident for older Alus (sequence divergence > 4%). We did a similar age segmentation analysis on RP pseudogenes, results shown in Table 6. (The numbers in the table were not normalized by amount of DNA.) We found different results for young pseudogenes than found above for young Alus. For young pseudogenes, there is no indication of enrichment in the GC-poor region (where "young" here is defined as sequence divergence less than 2% from their parents, the same cutoff as used in the study of the Alus). Note, however, there is a slight enrichment for the youngest pseudogenes, which have sequence divergence less than 1%, corresponding to roughly 6.7 Myr old. We think the reason we did not observe the same behavior for young pseudogenes as for young Alus is because of the much smaller sample size for pseudogenes. Also the recent decline in retrotransposition activity in human genome (Figure 5) (Lander *et al.* 2001) could have further complicated the situation as fewer fresh pseudogenes were generated in human genome.

Zhang *et al.*

In conclusion, the precise mechanism behind the negative correlation between gene GC content and processed pseudogene abundance remains unsettled until more pseudogene sequences from other protein families are available. Meanwhile, based on the analysis on Alu elements and the elimination of positive selection mechanisms for RP pseudogenes, the negative selection mechanism appears attractive.

METHODS

Figure 8A is a flow chart describing the basic procedures in finding RP pseudogenes.

Six-frame BLAST Search For Raw Fragment Homologies

We used the August 6, 2001 freeze of human genome draft, downloaded from Ensembl website (<http://www.ensembl.org>). Subsequently all the chromosomal coordinates were based on these sequences. The amino acid sequences of the 79 ribosomal proteins were extracted from SWISSPROT (Bairoch & Apweiler 2000). Since the sequence identity between the two RPS4 isoforms (RS4_HUMAN and RS4Y_HUMAN) is very high (91%), only protein RS4_HUMAN was used in the BLAST search. Each human chromosome was split into smaller overlapping chunks of 5.1 million bp, and tblastn program of the BLAST package 2.0 (Altschul *et al.* 1997) was run on these sequences. The genome sequence was not repeat-masked (Smit & Green) because we were concerned that some of the RP pseudogenes may reside in repetitive regions. Default SEG (Wootton & Federhen 1993) low-complexity filter parameters (12 2.2 2.5) were used in the homology search. We then picked the significant homology matches (e-value < 1E-4), and reduced them for mutual overlap by selecting the matches in decreasing order of

significance and removing any matches that overlap substantially with a picked match (i.e. more than 10 amino acids or 30 base pairs).

Merging Adjacent Fragment Homologies Into Single RP Matches

After sorting the BLAST matches according to their starting coordinates on the chromosomes, we found many neighboring matches on the same chromosome that match to the same RP. Some of these adjacent matches obviously were separate genes or pseudogenes, whereas others appeared to be part of the same gene or pseudogene. A two-step procedure was developed to determine (i) whether the neighboring matches belong to the same gene structure and (ii) whether they should be merged together into a longer homology match.

Step (i): Consider two adjacent homology fragments, M1 and M2, which are on the same chromosomal strand and match to the same RP (Figure 8B). M1 has chromosomal coordinates (c_{11}, c_{12}) and matches to amino acid sequence (q_{11}, q_{12}) on the query RP protein. Similarly, M2 has chromosomal coordinates (c_{21}, c_{22}) and matches to amino acids (q_{21}, q_{22}) on the query protein. By convention, q_{21} is always greater than q_{11} and c_{21} always greater than c_{12} . If M1 and M2 satisfy following two criteria, then we decide they belong to the same gene structure, i.e. they are either two exons of the same gene or two fragments of the same pseudogene interrupted by insertions.

(1) $|q_{21} - q_{12}| \leq \max(20, 0.2 \times L)$ and (2) $c_{21} - c_{12} \leq 5000$ (L denotes the length of the query RP peptide sequence). The reasoning behind criterion (1) is that if the two homology fragments have too much overlap or have too long a gap between them on the query protein sequence, then they should be considered as two separate and independent matches. Criterion (2) sets the maximum length of insertions in the middle of a pseudogene. We have checked that the introns in the RP genes are all shorter than 5000 bp, so we would not have accidentally split a gene into two.

Zhang *et al.*

Step (ii): If two homology fragments are determined to be part of the same gene or pseudogene structure in step (i), then in step (ii) the fragments were merged only if the chromosomal distance between the matches was shorter than 60 bp, i.e. $c_{22}-c_{21} \leq 60$. The rationale behind such treatment is: if the gap between the matches were too long then merging them together would generate errors in the Smith-Waterman re-alignment procedure described below. Also it has been shown that more than 95% of the introns in human are longer than 60 bp (Lander *et al.* 2001), so we wouldn't have accidentally merged two exons together or included introns into the coding sequence.

Optimization From Smith-Waterman Alignment of Merged Matches

After merging, each match was extended on both sides to equal the length of the RP they matched to, plus a buffer of 30 bp. For each extended match, the corresponding SWISSPROT protein sequences were then re-aligned to the genomic DNA sequence following the Smith-Waterman algorithm (Smith & Waterman 1981) by using the program FASTA (Pearson 1997). The reason for such an extension procedure is that BLAST may have skipped low-complexity segments in the query RP sequence; also, BLAST does not recognize frame shifts. After the re-alignment, the matches are "cleaned up": any redundant matches were removed; matches that contain gaps longer than 60 bp were split up into two individual matches. Since sequence alignment programs sometimes tend to pick up some extra residues at the ends of the alignment, each alignment was filtered to remove dubious matches at the ends. At this step, we had a total of 2531 pseudogene candidates in the whole genome that matched to the human RPs. Most of these were potential pseudogenes, but there could also be real functional RP genes in this set since we did not exclude any matches based on disablement.

Zhang *et al.*

Deriving a Set of RP Genes From Ensembl Database

We wanted to compare our pseudogene sets with the RP genes from Ensembl database (<http://www.ensembl.org>) (Birney *et al.* 2001; Hubbard *et al.* 2002). As of end of February 2002, there were approximately 47,000 confirmed genes, each with an annotated function. (Details regarding the Ensembl annotation procedure can be found in the aforementioned references.) We searched Ensembl database and picked out 549 genes that have been annotated as ribosomal proteins. Next we re-annotated these genes by aligning them pair-wise with human RP protein sequences, and picked out those Ensembl genes that had FASTA e-values lower than 0.0001. After removing a few remaining mitochondrial ribosomal protein genes, we had a set of 481 Ensembl nuclear RP genes.

While examining these Ensembl RP entries, it became obvious that most of these were pseudogenes other than real functional RP genes since they do not contain introns. 474 out of 481 (98.5%) Ensembl RP genes have significant overlaps with our pseudogene sets. Five single-exon RPL41 pseudogenes from Ensembl were added into our pseudogene sets.

Assessing For Processing By Checking for Exon Structures

We divided our pseudogene population into two subsets based on whether they contained long gaps in the middle of the sequence (Figure 8A). We labeled those pseudogenes as “processed” if they met two criteria: (i) they contained gaps of shorter than 60 bp, i.e. $c_{21}-c_{12} \leq 60$ in Figure 8B and (ii) they produced transcripts longer than 70% of the ribosomal protein they matched to. Venter *et al.* also previously used the last criterion (Venter *et al.* 2001). We also checked in GenBank that all 79 ribosomal protein genes contain introns longer than 60 bp. The remaining single-exon pseudogenes, which are shorter than 70% of the full-length protein, were labeled as

Zhang *et al.*

“fragments”. A total of 1912 “intact” processed pseudogenes and 358 pseudogenic fragments were identified at this step.

For those pseudogene candidates that contained multiple segments separated by gaps longer than 60 bp (total of 266), it was not straightforward to determine whether they were of processed or non-processed origin because the gaps could be either introns or repeat insertions. It is also likely that there were real functional ribosomal protein genes in this group. The cytogenetic locations of the 80 human RP genes (including the isoform gene RPS4Y on chromosome Y) have been previously mapped (Kenmochi *et al.* 1998; Uechi *et al.* 2001; Yoshihama *et al.* 2002). Using the cytogenetic map as reference and comparing the position of the gaps in the sequence with the exon structure of the functional RP genes, we identified 72 functional RP genes, 16 duplicated genes and assigned remaining 178 as “disrupted” processed pseudogenes. In summary, at the end of this process we had 2090 processed pseudogenes, 358 pseudogenic fragments, 72 functional RP genes and 16 duplicated RP genes.

Further Verification of Processing by Poly-A signal

When processed pseudogenes were integrated into genome from mRNA, a polyadenine tail at the 3' end would also be included (Mighell *et al.* 2000; Vanin 1985). This poly-adenine tail is at least 15-20 nucleotides long and is preceded by a polyadenylation signal (mostly AATAAA) (Wool *et al.* 1995). We were interested to survey how many of the ribosomal pseudogenes still had the polyadenine tail. Following the procedure previously described by Harrison *et al.* (Harrison *et al.* 2001), we searched a 1000 bp region that was 3' to the pseudogene homology segment, with a sliding window of 50 nucleotides for a region of elevated polyadenine content (>30 bp), and picked the most adenine-rich 50 bp segment as the most likely candidate. An interval of 1000 nucleotide was used because of the possible existence of 3'-untranslated regions (3'-UTRs); 90% of 3'-UTRs are of length less than 942 bp (Makalowski *et al.* 1996). In addition, we searched

Zhang *et al.*

in the same 1000 bp region for candidate AATAAA or other polyadenylation signals and checked whether they were upstream to the candidate polyadenine tail site.

Dating Processed Pseudogenes

Processed pseudogene sequences are aligned together with the corresponding functional RP gene sequences using program ClustalW (Thompson *et al.* 1994). For each pseudogene, we calculated sequence divergence from the present-day RP gene by program MEGA2 (Kumar *et al.* 2001), using Kimura 2-parameter model and pair-wise deletion. Kimura's 2-parameter model (Kimura 1980) corrects for transitional and transversional substitution rates while assuming that the four nucleotide-frequencies are the same and rates of substitution do not vary among sites. Evolutionary ages were calculated by the formula $T = D/k$, where D is the corrected divergence rate and k is the mutation rate per year per site for non-functional sequences. A mutation rate of 1.5×10^{-9} per site per year (Li 1997) was used.

Calculating Pseudogene Density In Different GC Region

Each human chromosome was divided into consecutive 100K bp long, non-overlapping segments. The GC content for each segment was calculated and the segment was assigned to one of the five groups according to their GC content: <37%, 37-41%, 41-46%, 46-52% and >52%. Number of processed pseudogenes in each group was counted and the pseudogene density for each group was calculated. Note we used the same GC content that Bernardi *et al.* used for isochores classification (Bernardi 2000; Macaya *et al.* 1976), although the validity of the isochore definition has been under debate (Bernardi 2001; Lander *et al.* 2001).

Zhang *et al.*

Expression Analysis

To investigate the possible correlation between the pseudogene abundance and the mRNA expression level, we compared the number of processed pseudogenes for each functional RP gene with its cellular mRNA expression level in the human cell (Yuval Kluger, personal communication) and the yeast cell (Cho *et al.* 1998). No significant correlation was found. Ribosomal protein genes are the most highly expressed genes in the cell; it is likely, in this case, the over abundance of mRNA transcripts has made the expression level a non-deciding factor for RP pseudogene retrotransposition.

ACKNOWLEDGEMENTS

The authors thank Adam Pavlicek for carefully reading the manuscript, and Arian Smit for providing the data on Alu/LINE sequence divergence. MG acknowledges NIH CEGS grant (P50 HG02357-01) for financial support. ZZ acknowledges Ted Johnson for doing the blast runs and thanks Paul Bertone, Ronald Jansen, Nick Luscombe, Yuval Kluger and Jiang Qian for helpful discussions.

REFERENCES

- Altschul S. F., Madden T. L., Schaffer A. A., Zhang J., Zhang Z., Miller W., and Lipman D. J. 1997. Gapped BLAST and PSI-BLAST: a new generation of protein database search programs. *Nucleic Acids Res.* **25**: 3389-402.
- Bairoch A., and Apweiler R. 2000. The SWISS-PROT protein sequence database and its supplement TrEMBL in 2000. *Nucleic Acids Res.* **28**: 45-8.
- Ban N., Nissen P., hansen J., Moore P. B., and Steitz T. 2000. The complete atomic structure of the large ribosomal subunit at 2.4 Å resolution. *Nature.* **400**: 841-7.
- Bernardi G. 2000. Isochores and the evolutionary genomics of vertebrates. *Gene.* **241**: 3-17.
- Bernardi G. 2001. Misunderstandings about isochores. Part 1. *Gene.* **276**: 3-13.
- Birney E., Bateman A., Clamp M. E., and Hubbard T. J. 2001. Mining the draft human genome. *Nature.* **409**: 827-8.
- Burge C., and Karlin S. 1997. Prediction of complete gene structures in human genomic DNA. *J. Mol. Biol.* **268**: 78-94.
- Cho R. J., Campbell M. J., Winzeler E. A., Steinmetz L., Conway A., Wodicka L., Wolfsberg T. G., Gabrielian A. E., Landsman D., Lockhart D. J., et al. 1998. A genome-wide transcriptional analysis of the mitotic cell cycle. *Mol Cell.* **2**: 65-73.
- Comtesse N., Reus K., and Meese E. 2001. The MGEA6 multigene family has an active locus on 14q and at least nine pseudogenes on different chromosomes. *Genomics.* **75**: 43-8.
- Crollius H. R., Jaillon O., Bernot A., Dasilva C., Bouneau L., Fisher C., Fizames C., Wincker P., Brottier P., and Quetier F. 2000. Estimate of human gene number provided by genome-wide analysis using Tetraodon nigroviridis DNA sequence. *Nature Genet.* **25**: 235-238.

Zhang *et al.*

- Draptchinskaia N., Gustavsson P., Andersson B., Pettersson M., Willig T. N., Dianzani I., Ball S., Tchernia G., LKlar J., and Matsson H. 1999. The gene encoding ribosomal protein S19 is mutated in Diamond-Blackfan anaemia. *Nature Genet.* **21**: 169-75.
- Esnault C., Maestre J., and Heidmann T. 2000. Human LINE retrotransposons generate processed pseudogenes. *Nature Genet.* **24**: 363-7.
- Ewing B., and Green P. 2000. Analysis of expressed sequence tags indicates 35,000 human genes. *Nature Genet.* **232**: 232-233.
- Eyre-Walker A. 1999. Evidence of selection on silent site base composition in mammals: potential implications for the evolution of isochores and junk DNA. *Genetics.* **152**: 675-83.
- Feng Q., Moran J. V., LKazazian H. H., and Boeke J. D. 1996. Human L1 retrotransposon encodes a conserved endonuclease required for retrotransposition. *Cell.* **87**: 905-16.
- Feo S., Davies B., and Fried M. 1992. The mapping of seven intron-containing ribosomal protein genes shows they are unlinked in the human genome. *Genomics.* **13**: 201-7.
- Fujii G. H., Morimoto A. M., Berson A. E., and Bolen J. B. 1999. Transcriptional analysis of the PTEN/MMAC1 pseudogene, psiPTEN. *Oncogene.* **18**: 1765-9.
- Glusman G., Yanai I., Rubin I., and Lancet D. 2001. The complete human olfactory subgenome. *Genome Res.* **11**: 685-702.
- Goncalves I., Duret L., and Mouchiroud D. 2000. Nature and structure of human genes that generate retropseudogenes. *Genome Res.* **10**: 672-8.
- Goodman M., Porter C. A., Czelusniak J., Page S. L., Schneider H., Shoshani J., Gunnell G., and Groves C. P. 1998. Toward a phylogenetic classification of Primates based on DNA evidence complemented by fossil evidence. *Mol. Phylogenet. Evol.* **9**: 585-98.
- Harrison P. M., Hegyi H., Balasubramanian S., Luscombe N. M., Bertone P., Echols N., Johnson T., and Gerstein M. 2002a. Molecular fossils in the human genome: identification and analysis of the pseudogenes in chromosomes 21 and 22. *Genome Res.* **12**: 272-80.

Zhang *et al.*

- Harrison P. M., Hegyi H., Bertone P., Echols N., Johnson T., Balasubramanian S., Luscombe N., and Gerstein M. 2001. Molecular fossils in the human genome: Identification and analysis of processed and non-processed pseudogenes in chromosomes 21 and 22. *Genome Res.* **12**: 272-280.
- Harrison P. M., Kumar A., Lang N., Snyder M., and Gerstein M. 2002b. A question of size: the eukaryotic proteome and the problems in defining it. *Nucleic Acids Res.* **30**: 1083-90.
- Hohjoh H., and Singer M. F. 1996. Cytoplasmic ribonucleoprotein complexes containing human LINE-1 protein and RNA. *EMBO J.* **15**: 630-9.
- Hohjoh H., and Singer M. F. 1997a. Ribonuclease and high salt sensitivity of the ribonucleoprotein complex formed by the human LINE-1 retrotransposon. *J. Mol. Biol.* **271**: 7-12.
- Hohjoh H., and Singer M. F. 1997b. Sequence-specific single-strand RNA binding protein encoded by the human LINE-1 retrotransposon. *EMBO J.* **16**: 6034-43.
- Hubbard T., Barker D., Birney E., Camero G., Chen Y., Clark L., Cox T., Cuff J., Curwen V., Down T., et al. 2002. The Ensembl genome database project. *Nucleic Acids Res.* **30**: 38-41.
- Jurka J. 1997. Sequence patterns indicate an enzymatic involvement in integration of mammalian retrotransposons. *Proc. Natl. Acad. Sci.* **94**: 1872-7.
- Kazazian H. H., Jr., and Moran J. V. 1998. The impact of L1 retrotransposons on the human genome. *Nature Genet.* **19**: 19-24.
- Kenmochi N., Kawaguchi T., Rozen S., Davis E., Goodman N., Hudson T. J., Tanaka T., and Page D. C. 1998. A map of 75 human ribosomal protein genes. *Genome Res.* **8**: 509-23.
- Kenmochi N., Yoshihama M., Higa S., and Tanaka T. 2000. The human ribosomal protein L6 gene in a critical region for Noonan syndrome. *J. Human Genet.* **45**: 290-3.
- Kimura M. 1980. A simple method for estimating evolutionary rates of base substitutions through comparative studies of nucleotide sequences. *J. Mol. Evol.* **16**: 111-20.

Zhang *et al.*

- Kumar S., Tamura K., Jakobsen I. B., and Nei M. 2001. MEGA2: molecular evolutionary genetics analysis software. *Bioinformatics*. **17**: 1244-5.
- Lander E. S., Linton L. M., Birren B., Nusbaum C., Zody M. C., Baldwin J., Devon K., Dewar K., Doyle M., FitzHugh W., et al. 2001. Initial sequencing and analysis of the human genome. *Nature*. **409**: 860-921.
- Leibold D. M., Swergold G. D., Singer M. F., Thayer R. E., Dombroski B. A., and Fanning T. G. 1990. Translation of LINE-1 DNA elements in vitro and in human cells. *Proc. Natl. Acad. Sci.* **87**: 6990-4.
- Li W.-H. 1997. Molecular Evolution.
- Macaya G., Thiery J. P., and Bernardi G. 1976. An approach to the organization of eukaryotic genomes at a macromolecular level. *J. Mol. Biol.* **108**: 237-54.
- Mager W. H., Planta R. J., Ballesta J. G., Lee J. C., Mizuta K., Suzuki K., Warner J. R., and Woolford J. 1997. A new nomenclature for the cytoplasmic ribosomal proteins of *Saccharomyces cerevisiae*. *Nucleic Acids Res.* **25**: 4872-5.
- Makalowski W., Zhang J., and Boguski M. S. 1996. Comparative analysis of 1196 orthologous mouse and human full-length mRNA and protein sequences. *Genome Res.* **6**: 846-57.
- Martin S. L. 1991. Ribonucleoprotein particles with LINE-1 RNA in mouse embryonal carcinoma cells. *Mol. Cell Biol.* **11**: 4804-7.
- McCarrey J. R., Kumari M., Aivaliotis M. J., Wang Z., Zhang P., Marshall F., and Vandenberg J. L. 1996. Analysis of the cDNA and encoded protein of the human testis-specific PGK-2 gene. *Dev. Genet.* **19**: 321-32.
- Mighell A. J., Smith N. R., Robinson P. A., and Markham A. F. 2000. Vertebrate pseudogenes. *FEBS Lett.* **468**: 109-14.
- Moran J. V., S.E. H., Naas T. P., DeBerardinis R. J., Boeke J. D., and Kazazian H. H., Jr. 1996. High frequency retrotransposition in cultured mammalian cells. *Cell*. **87**: 917-27.

Zhang *et al.*

- Mouchiroud D., D'Onofrio G., Aissani B., Macaya G., Gautier C., and Bernardi G. 1991. The distribution of genes in the human genome. *Gene*. **100**: 181-7.
- Olsen M. A., and Schechter L. E. 1999. Cloning, mRNA localization and evolutionary conservation of a human 5-HT7 receptor pseudogene. *Gene*. **227**: 63-9.
- Pavlicek A., Jabbari K., Paces J., Paces V., Hejnar J., and Bernardi G. 2001. Similar integration but different stability of Alus and LINEs in the human genome. *Gene*. **276**: 39-45.
- Pearson W. R. 1997. Comparison of DNA sequences with protein sequences. *Genomics*. **46**: 24-36.
- Planta R. J., and Mager W. H. 1998. The list of cytoplasmic ribosomal proteins of *Saccharomyces cerevisiae*. *Yeast*. **14**: 471-7.
- Raue H. A., and Planta R. J. 1991. Ribosome biogenesis in yeast. *Prog. Nucleic. Acid. Res. Mol. Biol.* **41**: 89-129.
- Schlutzen F., Tocilj A., Zarivach R., Harms J., Gluehmann M., Janell D., Bashan A., Bartels H., Agmon I., Franceschi F., et al. 2000. Structure of functionally activated small ribosomal subunit at 3.3 angstroms resolution. *Cell*. **102**: 615-23.
- Smit A. F. 1999. Interspersed repeats and other mementos of transposable elements in mammalian genomes. *Curr. Opin. Genetics. Dev.* **9**: 657-63.
- Smit A. F., and Green P. unpublished data.
- Smith T. F., and Waterman M. S. 1981. Identification of common molecular subsequences. *J. Mol. Biol.* **147**: 195-7.
- Thompson J. D., Higgins D. G., and Gibson T. J. 1994. CLUSTAL W: improving the sensitivity of progressive multiple sequence alignment through sequence weighting, position-specific gap penalties and weight matrix choice. *Nucleic Acids Res.* **22**: 4673-80.
- Uechi T., Tanaka T., and Kenmochi N. 2001. A complete map of the human ribosomal protein genes: assignment of 80 genes to the cytogenetic map and implications for human disorders. *Genomics*. **72**: 223-30.

Zhang *et al.*

Vanin E. F. 1985. Processed pseudogenes: characteristics and evolution. *Annu. Rev. Genet.* **19**: 253-72.

Venter J. C., Adams M. D., Myers E. W., Li P. W., Mural R. J., Sutton G. G., Smith H. O., Yandell M., Evans C. A., and Holt R. A. 2001. The sequence of the human genome. *Science.* **291**: 1304-51.

Wei W., Gilbert N., Ooi S. L., Lawler J. F., Ostertag E. M., Kazazian H. H., Jr., Boeke J. D., and Moran J. V. 2001. Human L1 retrotransposition: cis preference versus trans complementation. *Mol. Cell Biol.* **21**: 1429-1439.

Weiner A. M. 1999. Do all SINES lead to LINES? *Curr. Biol.* **9**: 842-4.

Wimberly B. T., Brodersen D. E., Clemons W. M., Morgan-Warren R. J., Carter A. P., Vonnrhein C., Hartsch T., and Ramakrishnan V. 2000. Structure of the 30S ribosomal subunit. *Nature.* **407**: 323-339.

Wool I. G. 1996. Extraribosomal functions of ribosomal proteins. *TIBS.* **21**: 164-5.

Wool I. G., Chan Y. L., and Gluck A. 1995. Structure and evolution of mammalian ribosomal proteins. *Biochem. Cell Biol.* **73**: 933-47.

Wootton J. C., and Federhen S. 1993. Statistics of local complexity in amino acid sequences and sequence databases. *Comput. Chem.* **17**: 149-163.

Yeh R. F., Lim L. P., and Burge C. 2001. Computational inference of homologous gene structures in the human genome. *Genome Res.* **11**: 803-816.

Yoshihama M., Uechi T., Asakawa S., Kawasaki K., Kato S., Higa S., Maeda N., Minoshima S., Tanaka T., Shimizu N., et al. 2002. The human ribosomal protein genes: sequencing and comparative analysis of 73 genes. *Genome Res.* **12**: 379-390.

Yusupov M. M., Yusupova G. Z., Baucom A., Lieberman K., Earnest T. N., Cate J. H., and Noller H. F. 2001. Crystal structure of the ribosome at 5.5 Å resolution. *Science.* **292**: 868-9.

Zhang *et al.*

Zinn A. R., Page D. C., and Fisher E. M. 1993. Turner syndrome: the case of the missing sex chromosome. *TIG*. **9**: 90-3.

FIGURE LEGENDS

Figure 1 RP processed pseudogenes statistics. (A) Distribution of relative sequence length among processed pseudogenes. Relative sequence length is the ratio between the length of translated pseudogene and the length of the corresponding functional ribosomal protein. (B) Distribution of the DNA sequence identity between processed pseudogenes and the cDNA sequence of functional RP proteins. (C) Distribution of number of disablements among processed pseudogenes.

Figure 2 The human RP processed pseudogene population. 24 human chromosomes are shown vertically from left to right. Pseudogenes are represented as short blue horizontal bars (—), long thick orange horizontal bars (—) delimit centromere region. Circular filled red spheres (●) represent chromosome ends.

Figure 3 (A) Correlation between chromosome length and number of processed RP pseudogenes on them. Each filled diamonds (◆) represents a chromosome. The correlation between number of processed pseudogenes on each chromosome and chromosome length is 0.89, $P < 1E-8$. (B) Processed pseudogene density on each chromosome is correlated with the chromosome GC content. The correlation coefficient is 0.51, $P < 0.01$.

Figure 4 (A) Distribution of Alu elements, LINE elements, processed RP pseudogenes and functional RP genes among genomic regions of different GC-content. Because of their different abundance in genome, these four species are plotted on different scales: number per 10Kb for Alus and LINEs, number per Mb for RP pseudogenes and number per 100 Mb for functional RP genes. (B) The drift in GC content for RP processed pseudogenes. The filled diamonds (◆) represent the GC content of functional RP gene coding sequence (CDS); the filled black squares (■) represent the GC content of processed pseudogenes. The vertical bars are standard errors.

Figure 5 Distribution of sequence divergence for RP processed pseudogenes in comparison with Alu and LINE1 repeats. Pseudogenes and repeats were grouped into bins according to their sequence divergence from consensus sequences. Each increment in divergence represents roughly 6.6 Myr (Million years). The LINE and Alu data are from A. Smit (personal communication).

Figure 6 (A) Distribution of processed pseudogenes among RP genes. Bars of different shades represent different age groups. (B) Lack of correlation between mRNA transcript length and number of processed pseudogenes. The pseudogenes are grouped into bins according to the length of their mRNA transcripts. Vertical bars are standard errors. (C) Significant inverse correlation between GC-content of RP gene coding sequence (CDS) and number of processed pseudogenes for that RP. The RP genes are grouped into four bins according to their CDS GC content.

Figure 7 Amino acid sequence alignment of RPL26 genes from yeast, worm, fruit fly, rat, human and a processed pseudogene (chr16_RL26_5) found in the intron region of the human functional RPS2 gene. The residues highlighted in gray are those present in the pseudogene and also in both the mammalian and invertebrate proteins; the residues outlined in bold are those present in the pseudogene and the mammals but not in invertebrates. In the pseudogene sequence, * represents a stop codon, and underscored amino acid indicates an adjacent frame shift. Rat and human RPL26 have almost identical sequences except at position 100, where the rat protein and the pseudogene have an Arginine and human protein has a Histidine.

Figure 8 (A) A flow chart showing procedures in searching for RP pseudogenes in human genome. RP and Ψ G denote “ribosomal protein” and “pseudogene” respectively, S-W. denotes “Smith-Waterman”. The steps are as follows: 1) Six-frame BLAST run searching for RP homologies in human genome. 2) Merging and extension. BLAST hits were merged and extended on both sides to match the length of RP peptide sequence. 3) Smith-Waterman re-alignment. Extended homologies were re-aligned with RP sequence. 4) Comparing with Ensembl annotation. Five RPL41 pseudogenes from Ensembl were added to the set. Total 2536 PR genes or pseudogenes were identified. 5) Checking for long gaps. Among those homology sequences that contain gaps shorter than 60 bp: they were labeled as “intact processed pseudogenes” if they are longer than 70% of the full-length RP sequence, otherwise they were labeled as “pseudogenic fragments”. 6) Comparing with GenBank and cytogenic mappings. For those RP homologies that contain long gaps (> 60 bp), their sequences were compared with the RP exon structure from GenBank and their chromosomal locations were checked with cytogenic mapping. The homology sequences were assigned as functional RP genes, duplicated RP genes and “disrupted processed pseudogenes”. The later were processed pseudogenes whose sequences were interrupted by retrotransposons. (B) A schematic graph describing the considerations in merging two adjacent RP matches: M1 and M2. (c_{11}, c_{12}) and (c_{21}, c_{22}) are chromosomal coordinates for M1 and M2. (q_{11}, q_{12}) and (q_{21}, q_{22}) are corresponding regions on the query RP protein that they match to.

Table 1. Number of RP Pseudogenes on Each Chromosome

Chromosome	Chr. size (Mb)	Chr. GC content	Functional RP genes	Processed Pseudogenes			Pseudogenic fragments	Processed + fragments	Pseudogene density ^c
				Intact ^a	Disrupted ^b	Total			
1	257	0.41	5	202	21	223	35	258	1.00
2	242	0.4	4	144	8	152	30	182	0.75
3	205	0.39	7	119	6	125	12	137	0.67
4	192	0.37	3	86	9	95	19	114	0.59
5	186	0.39	3	107	11	118	19	137	0.74
6	179	0.39	4	139	6	145	26	171	0.96
7	163	0.4	0	94	8	102	22	124	0.76
8	146	0.39	4	94	9	103	21	124	0.85
9	132	0.41	4	70	6	76	11	87	0.66
10	142	0.41	1	92	10	102	10	112	0.79
11	142	0.41	6	85	8	93	12	105	0.74
12	141	0.4	4	119	7	126	15	141	1.00
13	116	0.38	1	43	3	46	10	56	0.48
14	106	0.41	1	78	10	88	17	105	0.99
15	100	0.42	3	55	7	62	10	72	0.72
16	93	0.44	3	44	9	53	16	69	0.74
17	84	0.45	6	80	11	91	13	104	1.24
18	82	0.39	1	43	2	45	5	50	0.61
19	77	0.47	13	66	8	74	16	90	1.17
20	63	0.44	1	44	3	47	12	59	0.94
21	45	0.41	0	21	0	21	6	27	0.60
22	48	0.48	1	25	6	31	6	37	0.77
X	152	0.39	4	61	8	69	15	84	0.55
Y	59	0.39	1 ^d	1	2	3	0	3	0.05
Total	3152	0.41	80	1912	178	2090	358	2448	0.78

^a Processed pseudogenes that are continuous in sequence with insertions ≤ 60 bp

^b Processed pseudogenes that are disrupted by insertions (> 60 bp)

^c Number of processed pseudogenes + pseudogenic fragments per 1 Mb DNA

^d RSP4Y on chromosome Y is an isoform of RSP4X on chromosome X

Correlation (chromosome size, number of processed pseudogenes) = 0.89, $P < 1E-8$

Correlation (chromosome size, number of processed pseudogenes + fragments) = 0.89, $P < 1E-8$

Table 2. Overall Statistics of RP Processed Pseudogenes

	Ave. Relative sequence length ^a	Ave. a.a. identity ^b	Ave. nt. identity ^c	Ave. disablements ^d	Ave. 5' truncation ^e	Ave. 3' truncation ^f
Processed pseudogenes	96.5%	76.2%	86.8%	3.6	13	8
Pseudogenic fragments	42.1%	74.2%	84.1%	2.0	227	127
Total	88.5%	75.9%	84.8%	3.4	44	26

^a Length of translated pseudogenes divided by the length of RP peptides, averaged over the entire pseudogene population.

^b Average sequence identity between translated pseudogene and RP peptide sequence.

^c Average sequence identity between pseudogene sequence and RP cDNA sequence.

^d Average number of premature stop codons, frame shifts, and repeat insertions in the processed pseudogenes

^e Average number of missing nucleotides at 5' end, CDS only.

^f Average number of missing nucleotides at 3' end, CDS only.

Table 3. Genomic Distribution of RP Processed Pseudogenes

	Genomic GC-content ^a					Total
	< 37%	37-41%	41-46%	46-52%	>52%	
Number of functional RP genes ^b	8	6	23	27	22	86
RP gene density (per 100 Mb)	0.98	0.61	3.2	8.3	23.4	2.73
Number of RP pseudogenes	310	601	804	318	57	2090
Pseudogene density (per 10 Mb)	3.8	6.1	11	9.7	6.1	6.63

^a Genomic regions grouped by their average GC content

^b Including duplicated copies of the functional RP genes

Table 4. Distributions of Processed Pseudogenes Among RP Genes

Gene name ^a	SWISSPROT ID ^b	mRNA length ^c	CDS length ^d	CDS GC content ^e	# Processed	# Fragments
RPL21	RL21_HUMAN	568	483	0.43	145	13
RPL23A	RL2B_HUMAN	546	471	0.49	85	11
RPL7	RL7_HUMAN	838	747	0.43	83	19
RPL7A	RL7A_HUMAN	890	801	0.54	73	13
RPL31	RL31_HUMAN	442	378	0.47	71	5
RPSA	RSP4_HUMAN	1039	888	0.53	67	12
RPS26	RS26_HUMAN	459	348	0.53	65	5
RPS3A	RS3A_HUMAN	921	795	0.43	60	15
RPL17	RL17_HUMAN	898	555	0.46	59	11
RPS2	RS2_HUMAN	978	882	0.58	57	10
RPL39	RL39_HUMAN	401	156	0.42	56	8
RPL36A	RL44_HUMAN	425	321	0.47	54	6
RPL12A	RL12_HUMAN	632	498	0.52	49	3
RPL34	RL34_HUMAN	849	354	0.45	44	3
RPS15A	RS1A_HUMAN	541	393	0.47	43	4
RPL29	RL29_HUMAN	737	480	0.56	40	3
RPL26	RL26_HUMAN	525	438	0.45	39	3
RPS27	RS27_HUMAN	344	255	0.49	38	0
RPL5	RL5_HUMAN	1033	894	0.44	37	8
RPS20	RS20_HUMAN	539	360	0.45	36	0
RPL35A	R35A_HUMAN	511	333	0.47	36	2
RPL32	RL32_HUMAN	521	408	0.51	36	7
RPS29	RS29_HUMAN	346	171	0.53	36	2
RPS12	RS12_HUMAN	534	399	0.46	33	8
RPS10	RS10_HUMAN	598	498	0.55	33	4
RPL9	RL9_HUMAN	716	579	0.44	31	6
RPS24	RS24_HUMAN	537	402	0.44	30	13
RPL6	RL6_HUMAN	950	867	0.47	30	5
RPS6	RS6_HUMAN	829	750	0.47	27	1
RPL37	RL37_HUMAN	371	294	0.51	27	3
RPL13A	R13A_HUMAN	1142	612	0.58	26	3
RPS27A	R27A_HUMAN	551	471	0.44	24	1
RPL36	RL36_HUMAN	428	318	0.6	24	2
RPS4	RS4_HUMAN	916	792	0.48	23	5
RPL22	RL22_HUMAN	574	387	0.44	22	1
RPL19	RL19_HUMAN	698	591	0.54	22	4
RPL15	RL15_HUMAN	2018	615	0.54	21	5
RPS7	RS7_HUMAN	729	585	0.48	18	5

RPS17	RS17_HUMAN	515	408	0.51	18	3
RPP1	RLA1_HUMAN	512	345	0.54	17	3
RPL18A	RL1X_HUMAN	618	531	0.6	17	7
RPL30	RL30_HUMAN	524	348	0.45	16	1
RPS16	RS16_HUMAN	570	441	0.57	16	1
RPL10A	R10A_HUMAN	700	654	0.51	14	4
RPL10	RL10_HUMAN	2188	645	0.55	14	32
RPL18	RL18_HUMAN	648	567	0.59	14	1
RPS18	RS18_HUMAN	549	459	0.56	13	3
RPL13	RL13_HUMAN	1110	636	0.62	13	1
RPL23	RL23_HUMAN	493	423	0.49	11	1
RPL27	RL27_HUMAN	513	411	0.49	11	4
RPS8	RS8_HUMAN	705	627	0.52	11	3
RPP0	RLA0_HUMAN	1116	954	0.54	11	4
RPS28	RS28_HUMAN	398	210	0.62	11	2
RPS5	RS5_HUMAN	725	615	0.58	10	1
RPS15	RS15_HUMAN	515	438	0.63	10	1
RPS23	RS23_HUMAN	506	432	0.45	9	1
RPS25	RS25_HUMAN	514	378	0.47	9	0
RPL37A	R37A_HUMAN	392	279	0.52	9	1
RPL40 ^f	RL40_HUMAN	501	387	0.54	9	1
RPS21	RS21_HUMAN	356	252	0.54	9	0
RPL3	RL3_HUMAN	1311	1212	0.55	9	5
RPL35	RL35_HUMAN	455	372	0.57	9	2
RPS13	RS13_HUMAN	529	456	0.46	8	4
RPL24	RL24_HUMAN	556	474	0.48	8	9
RPS14	RS14_HUMAN	589	456	0.54	8	2
RPP2	RLA2_HUMAN	482	348	0.56	8	0
RPL38	RL38_HUMAN	368	213	0.46	7	4
RPS3	RS3_HUMAN	843	732	0.54	7	3
RPL4	RL4_HUMAN	1449	1284	0.49	6	5
RPS11	RS11_HUMAN	594	477	0.51	6	3
RPL27A ^f	RL2A_HUMAN	514	447	0.54	6	5
RPS19	RS19_HUMAN	569	438	0.58	6	0
RPL28	RL28_HUMAN	500	414	0.6	6	1
RPL41	RL41_HUMAN	478	78	0.5	5	0
RPL11	RL11_HUMAN	609	537	0.51	4	3
RPS30 ^f	RS30_HUMAN	574	402	0.59	4	1
RPS9	RS9_HUMAN	691	585	0.6	4	1
RPL8	RL8_HUMAN	894	774	0.61	4	3
RPL14	RL14_HUMAN	843	651	0.5	3	3

Total	685	511	0.51	26	4.5
Correlation	-0.01 ^g	0.04 ^h	-0.41 ⁱ		
<i>p</i> -value	0.93	0.73	0.0002		

^a The SWISSPROT ID (Bairoch & Apweiler 2000) for the human RP protein

^b The standard mammalian RP gene nomenclature

^c Number of nucleotides for RP mRNA

^d Number of nucleotides for RP coding sequence (CDS)

^e GC content of the RP coding sequence

^f RPS27a, RPL40 and RPS30 are carboxyl extensions of ubiquitin or ubiquitin-like proteins.

^g Correlation between number of processed pseudogenes and mRNA length

^h Correlation between number of processed pseudogenes and CDS length

ⁱ Correlation between number of processed pseudogenes and CDS GC-content

Table 5. Duplicated Human RP genes

gene	Duplicated			Original ^a		
	Chr. location	Size (bp)	Ensembl ID	Chr. location	Size (bp)	Ensembl ID
RPS3A	4q31.23	4114	ENSG00000145425	4q31.23	4114	ENSG00000151940
RPL26	5q35.3	9664	ENSG00000037241	17p13.1	4743	ENSG00000161970
RPL8 (I) ^b	8q24.3	2287	ENSG00000130795	8q24.3	2287	ENSG00000147785
RPL8 (II)	8q24.3	2287	ENSG00000161009	8q24.3	2287	ENSG00000147785
RPL7A	9q34.3	1814	ENSG00000160312	9q34.3	1814	ENSG00000148303
RLP0 (I) ^c	12q24.31	3474	N/A ^d	12q24.23	3474	N/A
RLP0 (II) ^c	12q24.31	2182	ENSG00000123062	12q24.23	3474	N/A
RPS27	15q21.3	912	N/A	1q21.3	573	ENSG00000157616
RPS17 ^f	15q26.3	685	ENSG00000154241	15q25.2	3329	ENSG00000103720
RPL3	16p13.3	8650	ENSG00000140986	22q13.2	5402	ENSG00000100316
RPS15A	16p13.11	6100	ENSG00000157115	16p13.11	6100	ENSG00000134419
RPL17	18q21.1	2221	ENSG00000141618	18q21.1	2220	ENSG00000154807
RPL13A ^g	19q13.13	1016	N/A	19q13.33	1966	ENSG00000142541
RPS9	19q13.42	6385	ENSG00000131036	19q13.42	6385	ENSG00000074164
RPL36	19p13.3	1108	ENSG00000130255	19p13.2	1108	ENSG00000141995
RPS4Y	Yq11.222	24252	ENSG00000157828	Yp11.31	24727	ENSG00000129824

^a RP genes identified from hybridation experiments

^{b,c} Two copies of duplications are found for the same RP gene

^d Not present in Ensembl. (Jan. 2002 release)

^e This duplicated RP gene starts from amino acid 17

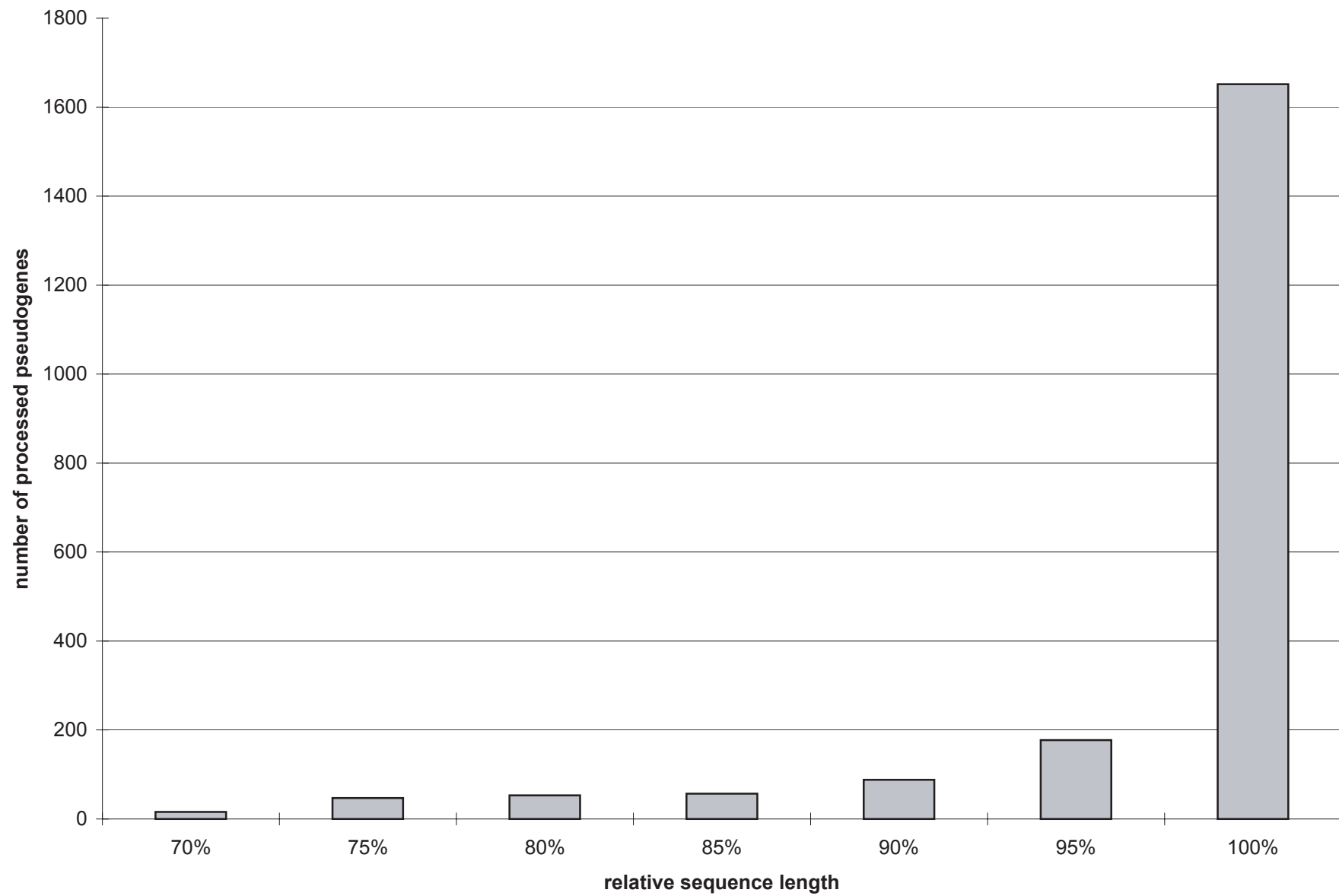
^f This duplicated RP gene only contain amino acids 50-138.

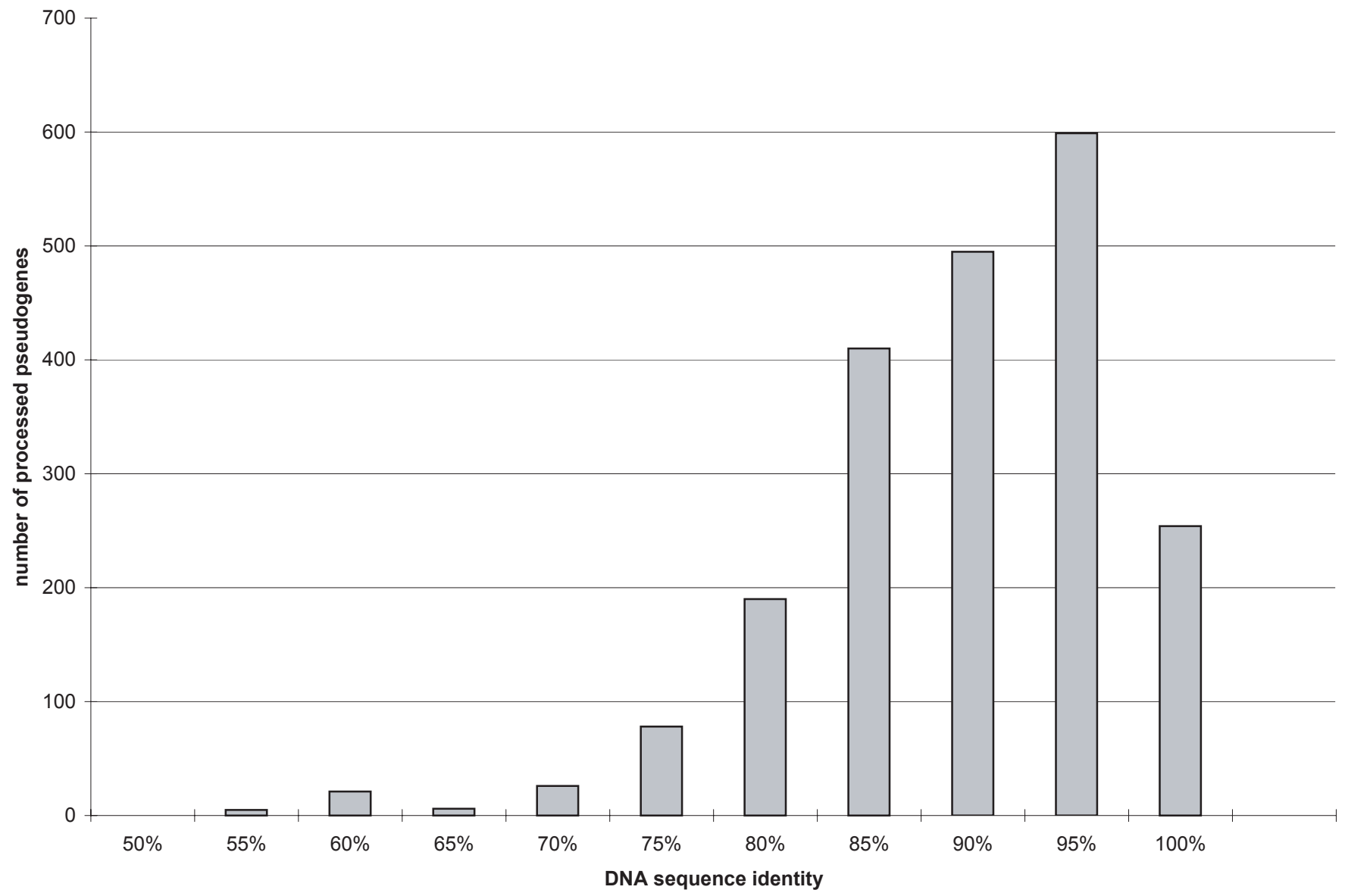
^g This duplicated RP gene has a frame shift

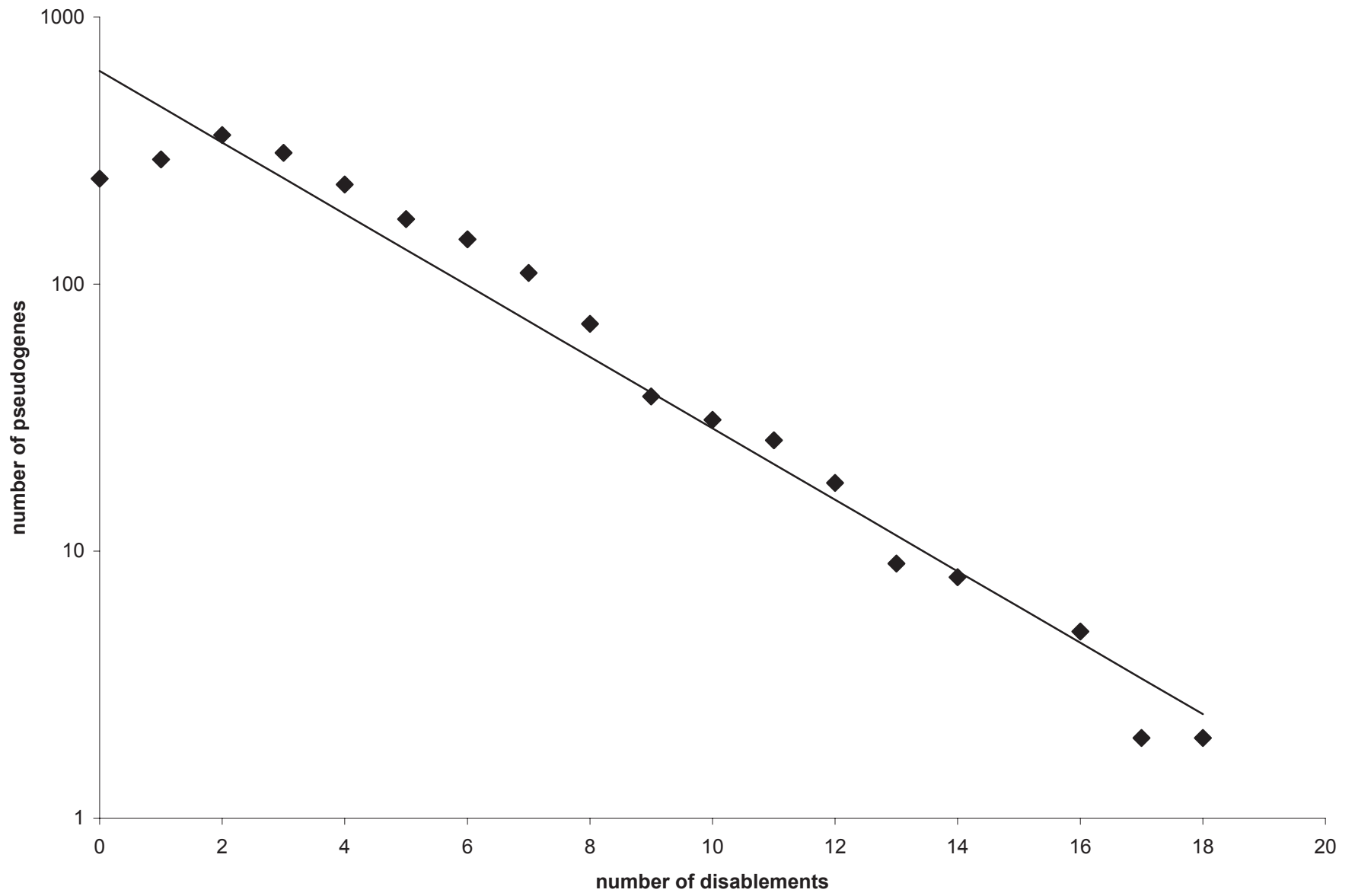
Table 6. Genomic Distributions of RP Pseudogenes of Different Ages

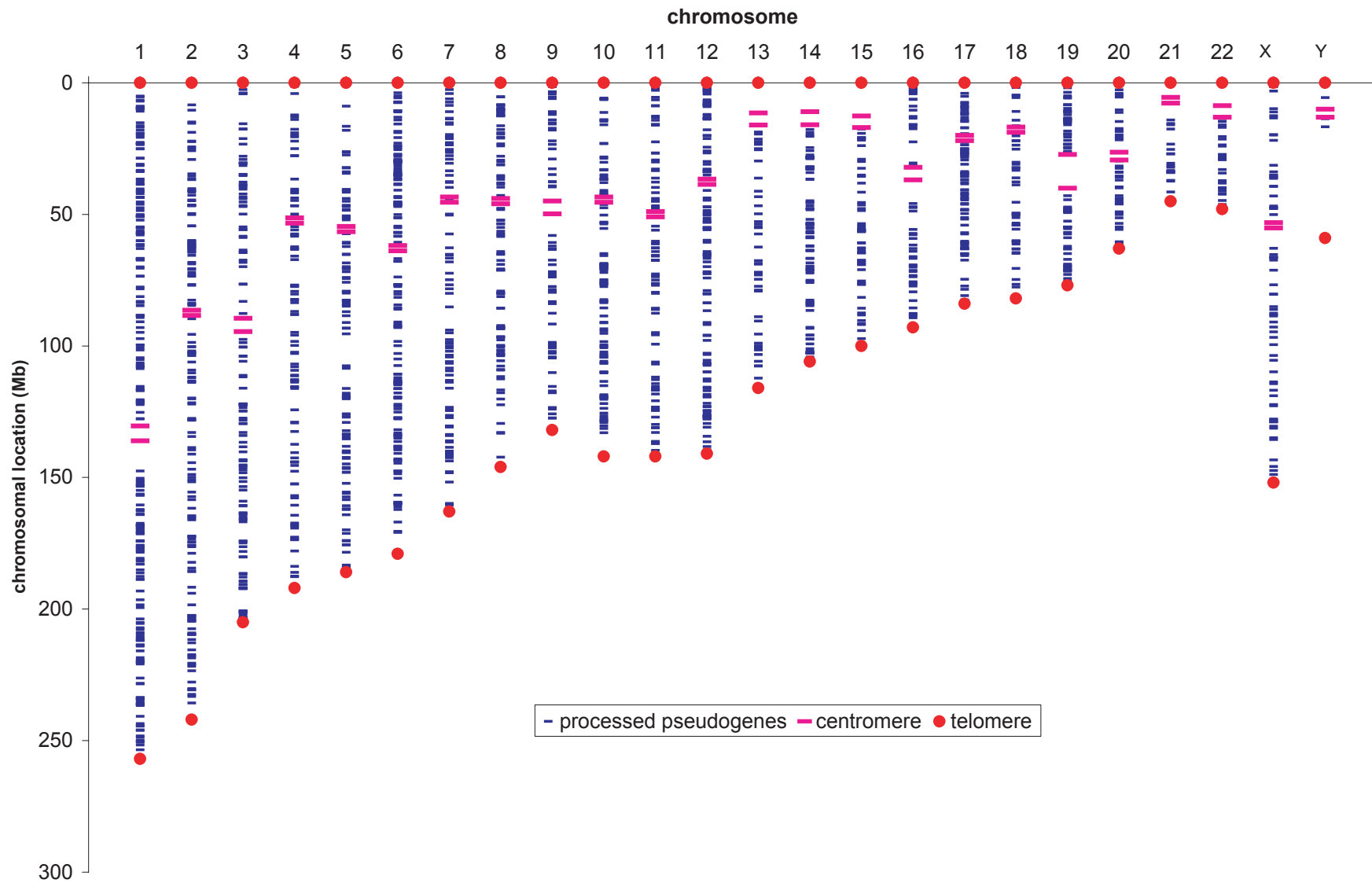
Sequence divergence	Number of pseudogenes in the genomic region ^a				
	<37%	37-41%	41-45%	45-52%	>52%
≤ 1%	4	12	12	8	2
≤ 2%	13	26	31	11	2
> 2%	303	575	768	306	55

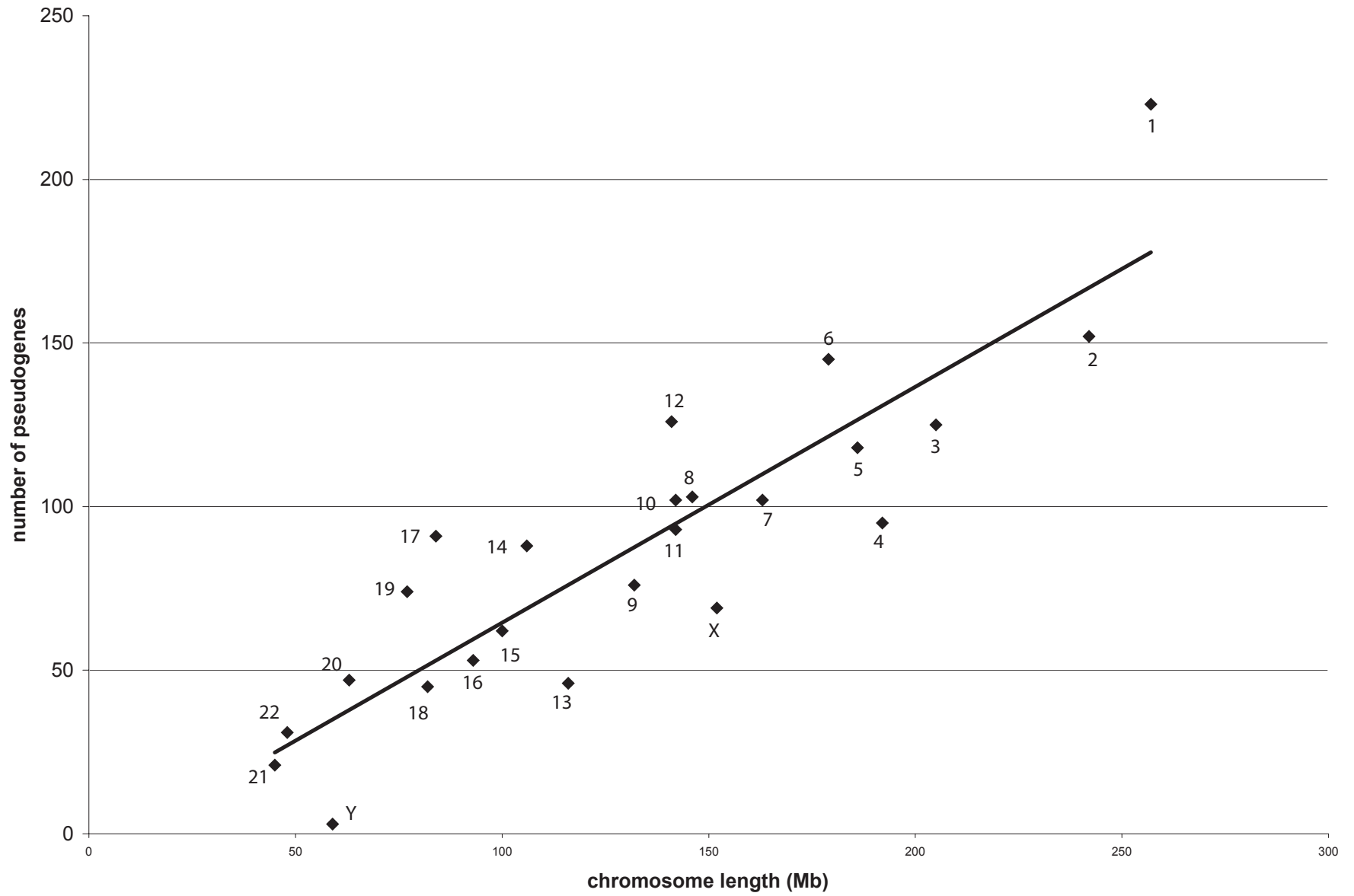
^a Genomic regions of 100 Kb long are binned by their average GC-content.

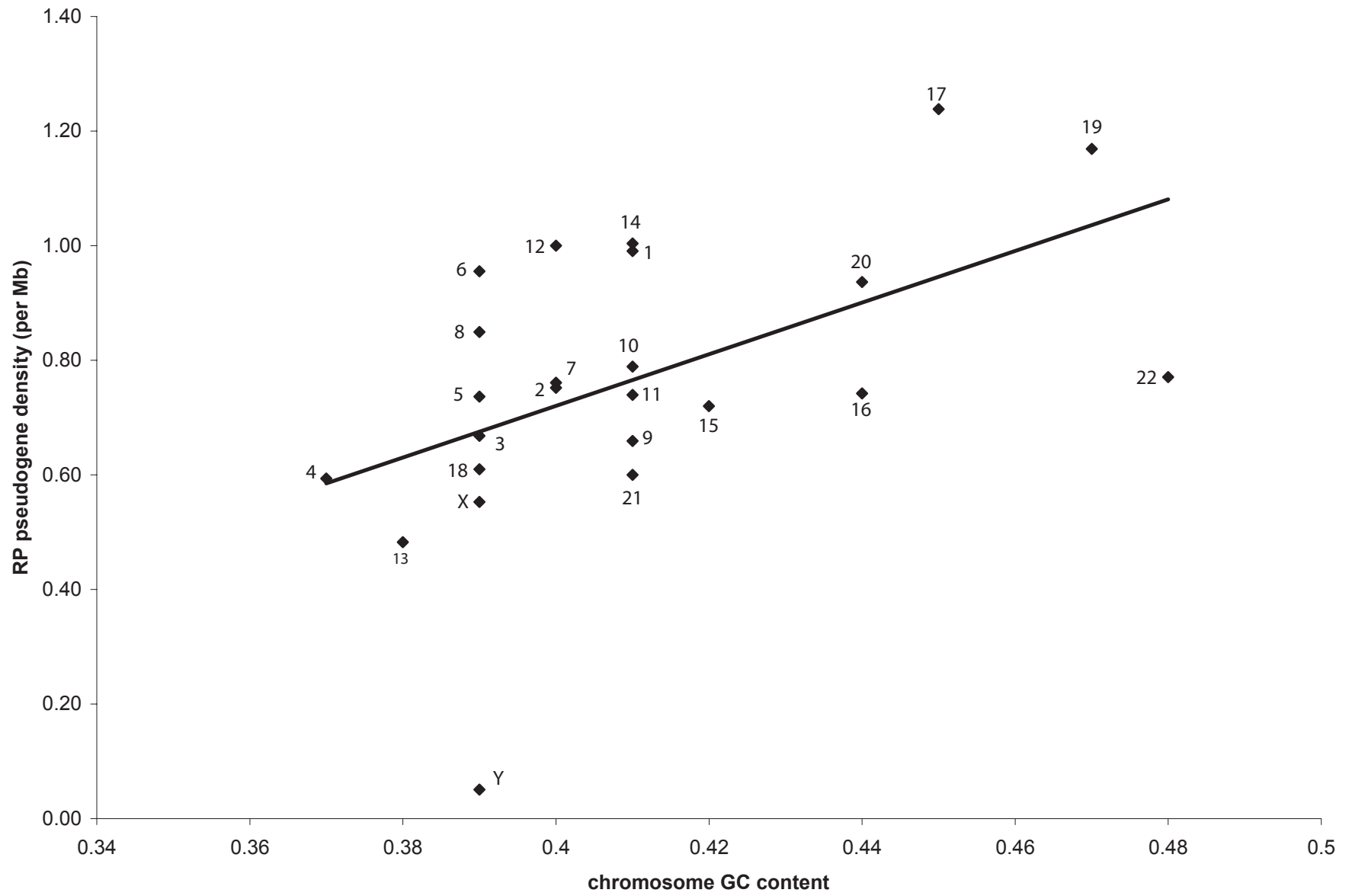


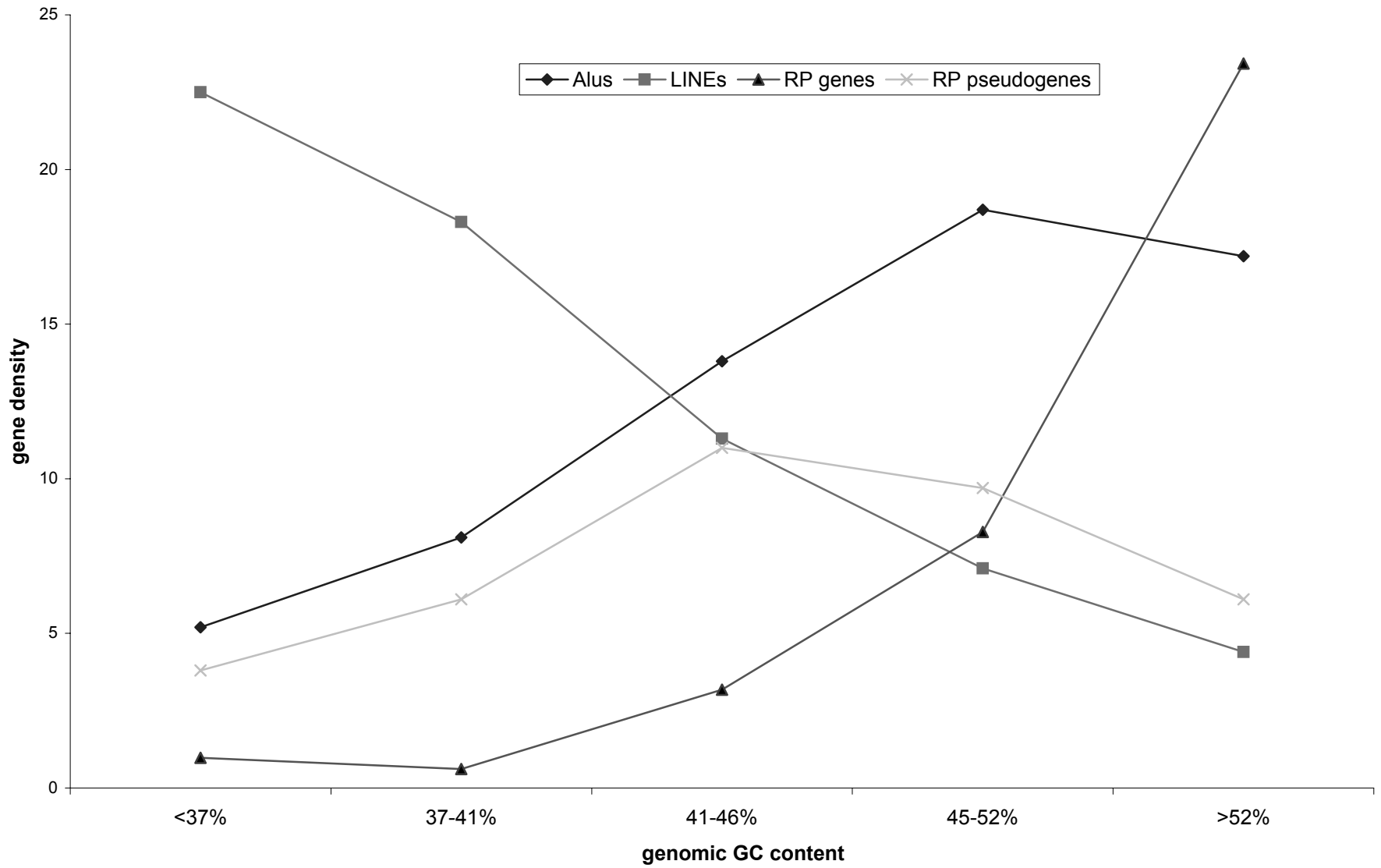


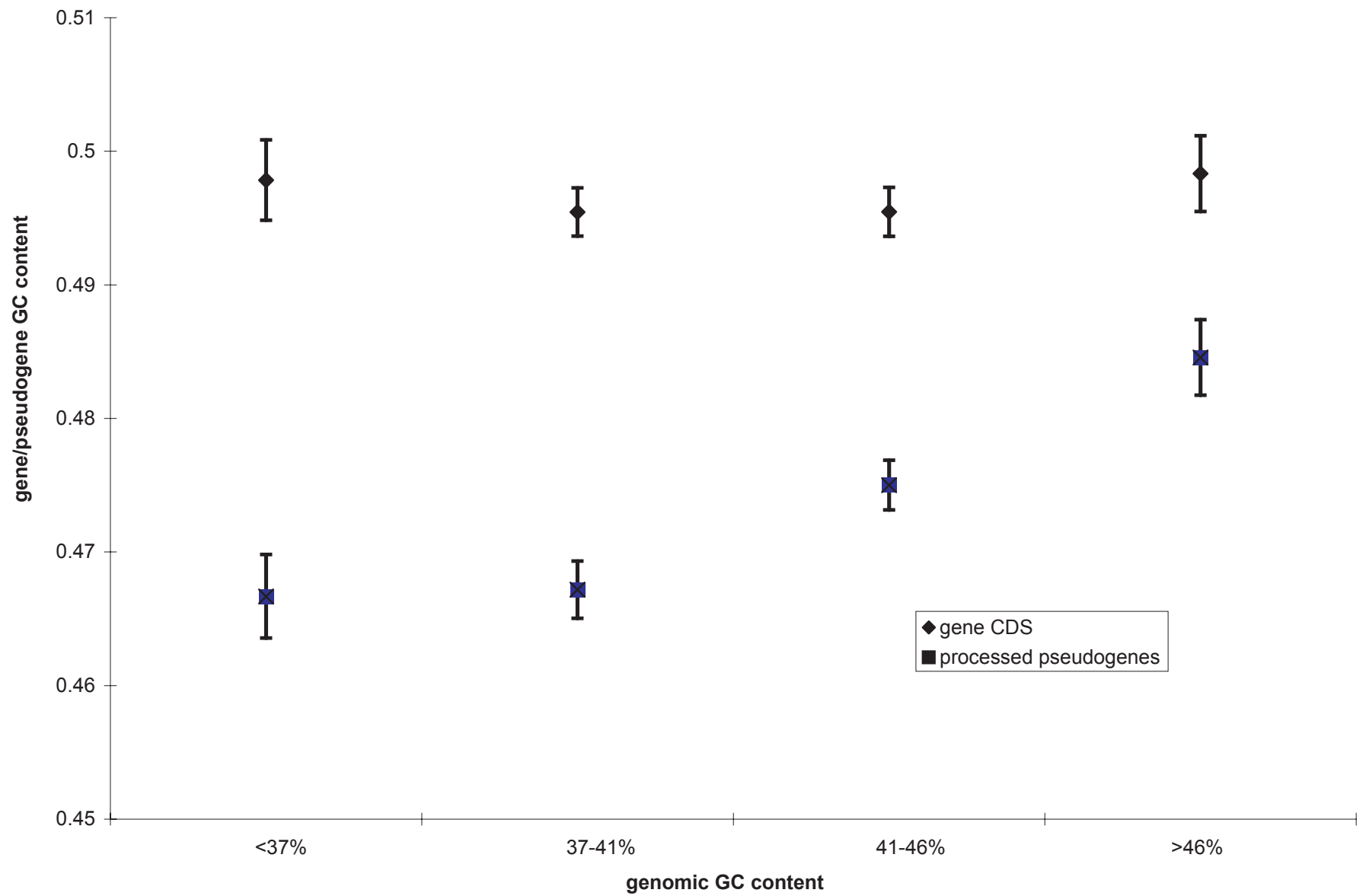


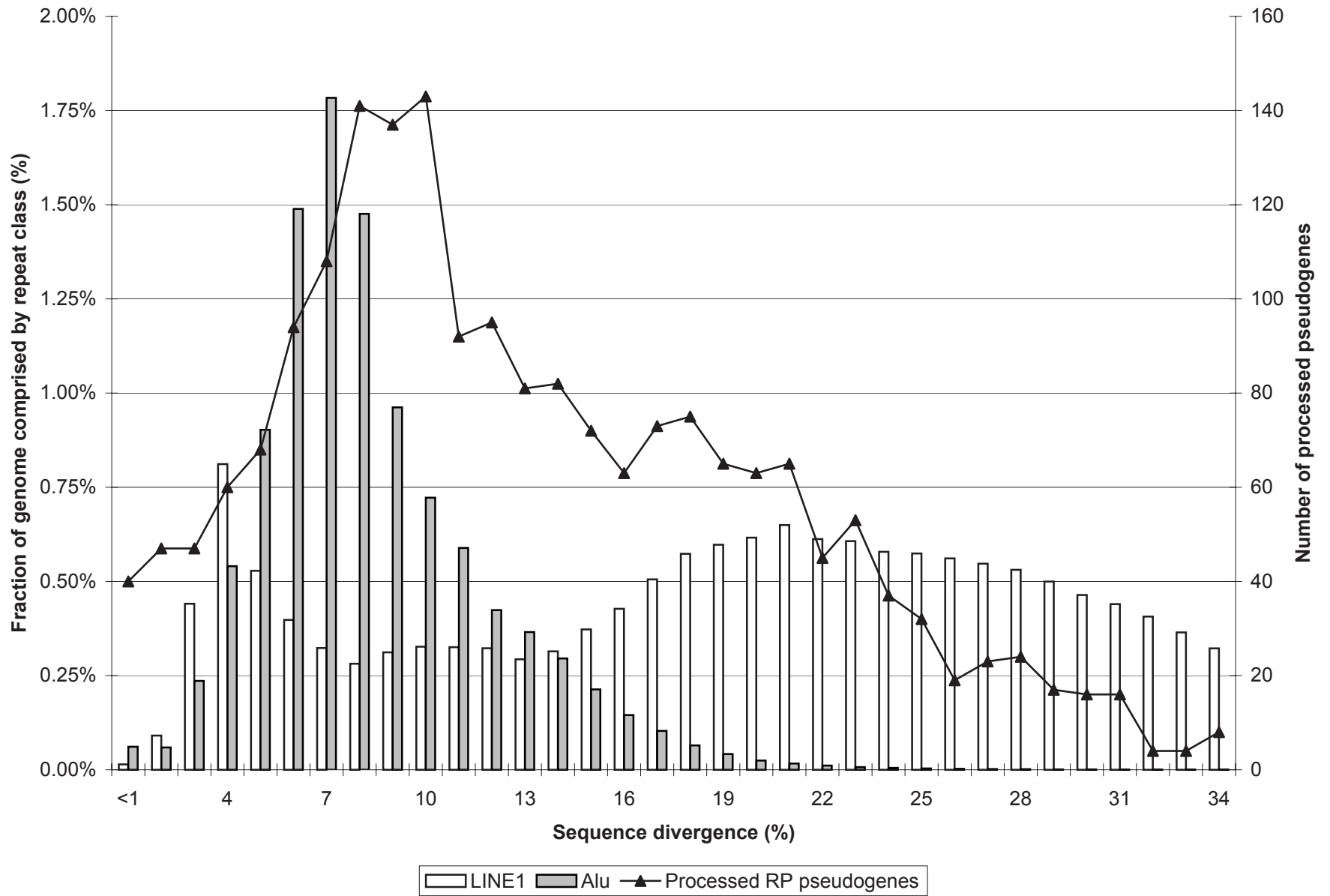


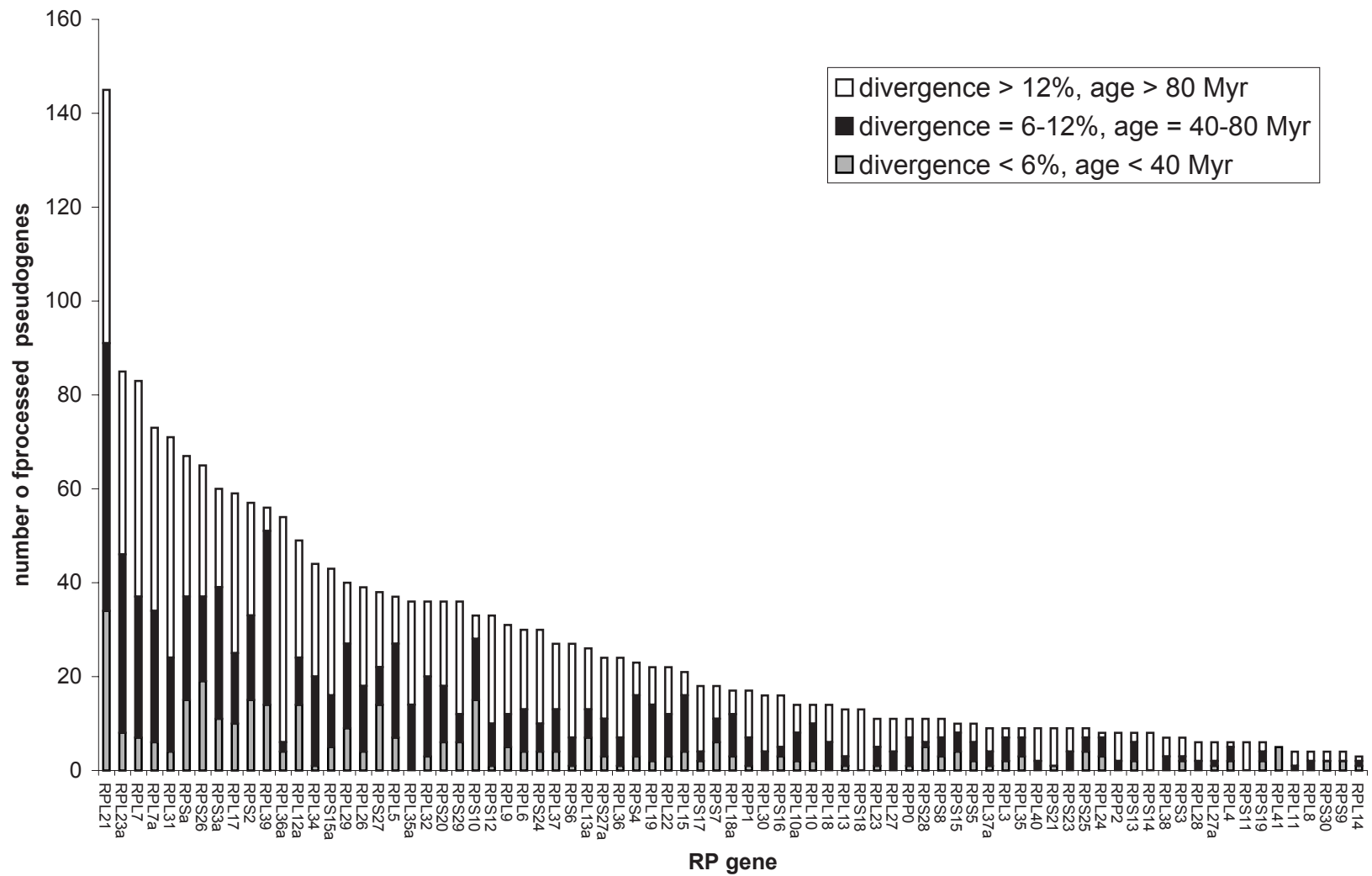


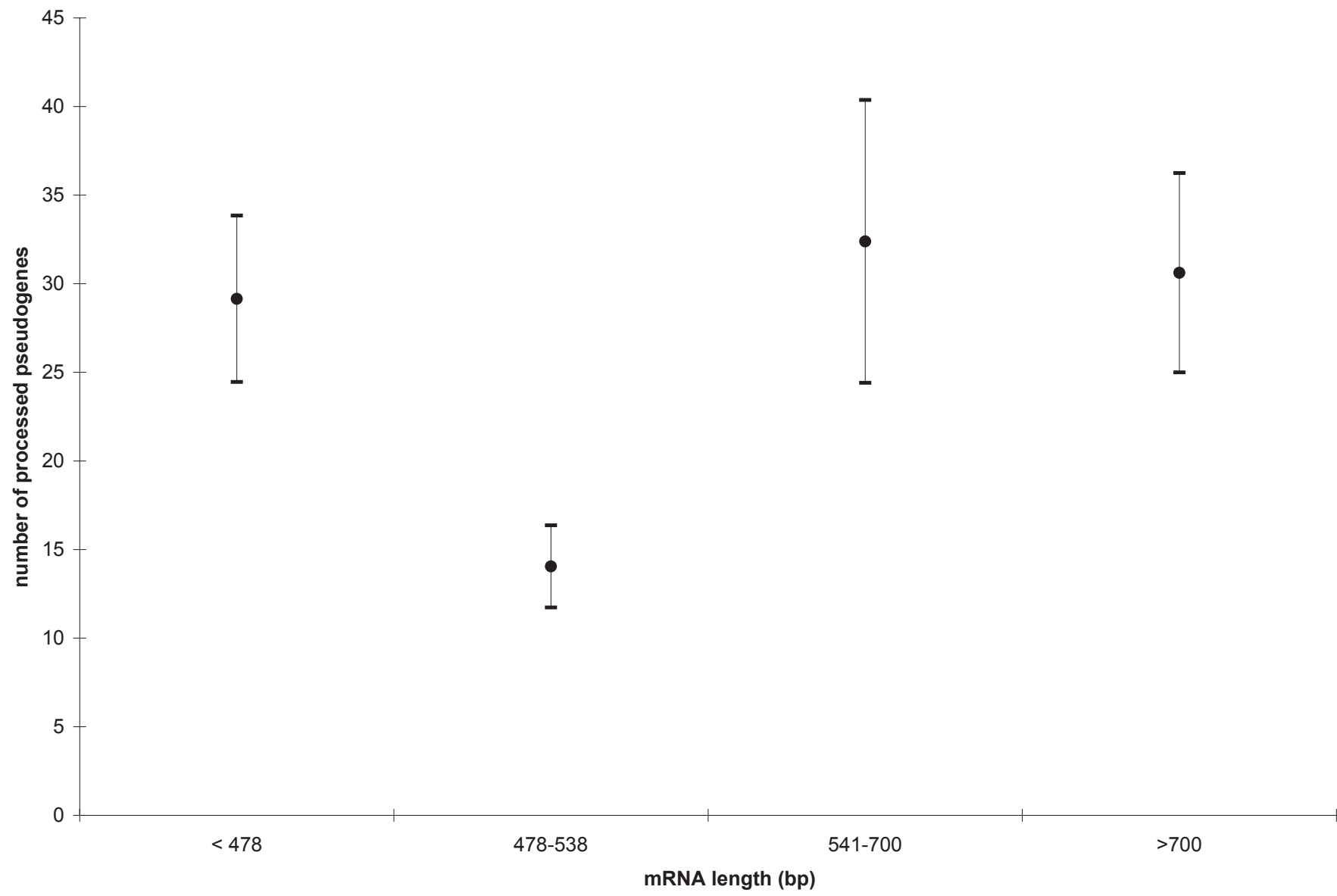


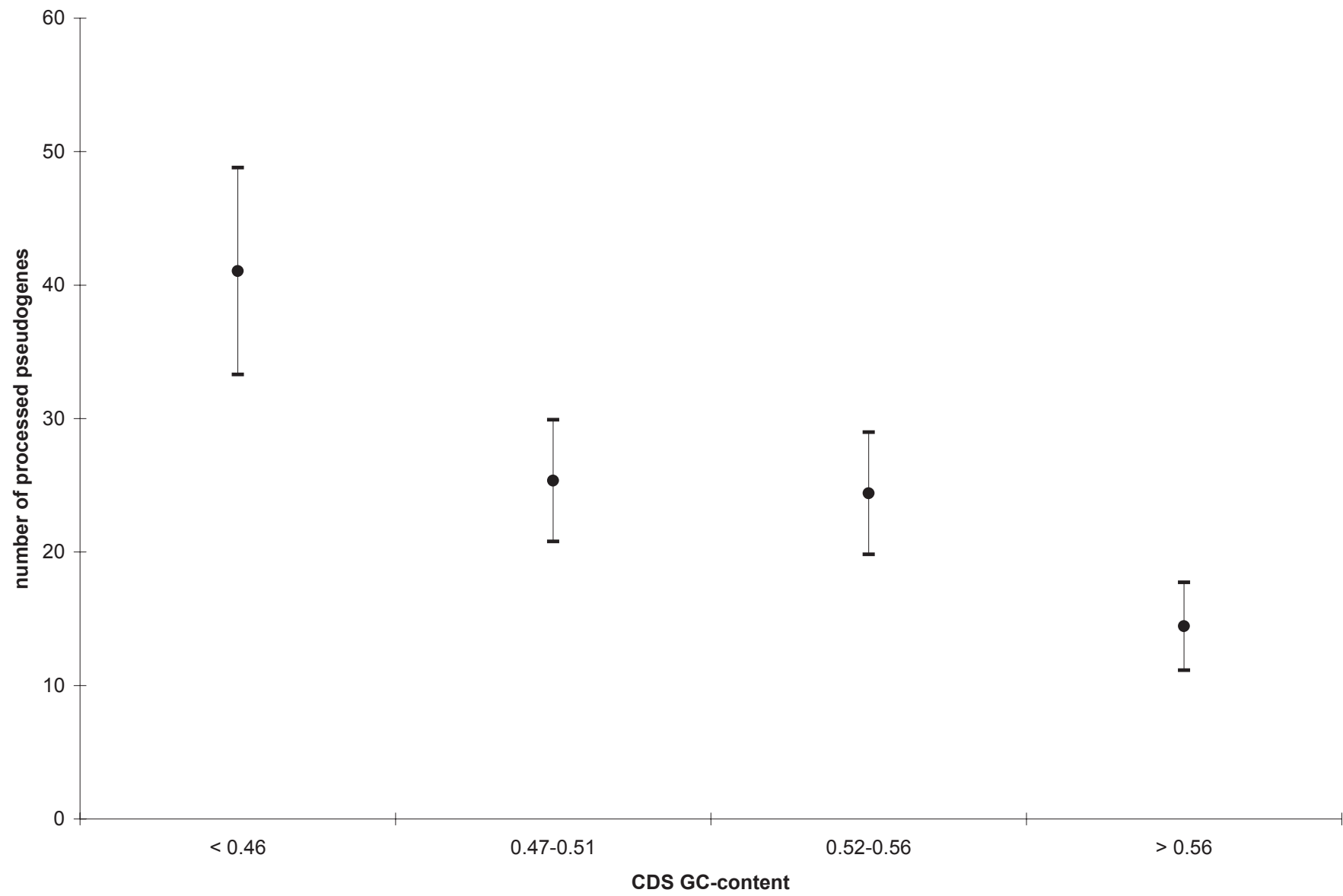












yeast	1	AKQSLDVSSDRRKARKAYFTAPSSQRRVLLSAPLSKELRAQYGIKALPIRR
worm	1	MKVNPFVSSDSGKSRKAHFNAPSHERRRIMSAPLTKELRTKHGIRAIPIRT
fruitfly	1	MKQNPVSSSRKNRKRHFQAPSHIRRLMSAPLSKELRQKYNVRSMPIRR
rat	1	MKFNPFVTSDRSKNRKRHFNAPSHIRRKIMS SPLSKELRQKYNVRSMPIRK
human	1	MKFNPFVTSDRSKNRKRHFNAPSHIRRKIMS SPLSKELRQKYNVRSMPIRK
chr16_RL26_5		- - - - - SHKRHFSASSHIRSEFISKELKEKQRLVH - - - - AIRE

100

yeast	61	SKKG - QEGKISSVYRLKFAVQVDKVTKEKVNGASVPINLHPS - - KLVITKL
worm	61	RHKG - NTGRVLR CYRKKFVIHIDKITREKANGSTVHIGIHPS - - KVAITKL
fruitfly	61	HFKGNQVGKVVQAYRKKFVVYVEKI QRENANGT NVYVGIHPS - - KVLIVKL
rat	61	HYKGQQIGKV VQVYRKKYVIYIERVQREKANGTTVHVGIHPS - - KVVITRL
human	61	HYKGQQIGKV VQVYRKKYVIYIERVQREKANGTTVHVGIHPS - - KVVITRL
chr16_RL26_5		HCKG - *QTVIVRVYG - TAVICIQRVQWGKANGTICHVSVRPSKVTVVMARP

yeast	118	IQRKG - - - - - GKLE - - - - -
worm	118	VERKAAGRSRVTGILKGGKHTDETVN - - - - -
fruitfly	119	LERRGKGR LAALGKDKGKYTEETA AQPMETA
rat	119	LERKAKSR - - QVGKEKGGKYKEETIEKMQE - -
human	119	LERKAKSR - - QVGKEKGGKYKEETIEKMQE - -
chr16_RL26_5		SGKPHLTK - - - - QEKKGK* - EETIE - - - - -

